ELSEVIER

Journal of Fluids and Structures 23 (2007) 365–389

JOURNAL OF FLUIDS AND STRUCTURES

www.elsevier.com/locate/jfs

Control with trim tabs and history-dependent aerodynamic forces

G. Iosilevskii*

Faculty of Aerospace Engineering, Technion, Haifa 32000, Israel

Received 25 February 2006; accepted 30 September 2006
Available online 13 December 2006

Abstract

This analytical study addresses three different, but closely related problems: time-history dependence of aerodynamic forces acting on a moving control surface, control by means of trim tabs, and control surface reaction upon abrupt actuator failure. Closed-form solutions are proposed to each of these problems. Perhaps the most conspicuous result is our conclusion that history-dependent aerodynamic effects have no significant influence on the transfer function between the trim tab and the surface it drives, provided that the chord of the surface is sufficiently small compared to the total chord.

Keywords: Unsteady aerodynamics; History-dependent forces; Control with tabs

1. Introduction

It is well known that any bending, twisting, flapping, control-surface-moving wing leaves a vortical wake behind it. Some of the vortices comprising the wake are associated with the finite span of the wing—those vortices are, loosely, parallel with the direction of the flow relative to the wing; other vortices are associated with wing motions—these are, loosely, perpendicular to the direction of the flow. As the latter are created any time there is a change in the flow about the wing, the wake records, in a way, the history of the wing motion. At the same time, the wake feeds back the flow around the wing, and thus affects the aerodynamic loads acting on it. Hence, aerodynamic loads are inherently history dependent.

Comprising an inseparable part of unsteady aerodynamic loads, history-dependent effects are well known in aeroelasticity (Bisplinghoff et al., 1996; Dowell et al., 1989). Our interest in these effects rose in the framework of ADFCS II project in the context of possible failures in aircraft control systems (many authors, 2000). In the event of a primary control surface actuation failure, either as a result of hydraulic pressure loss, or as a result of mechanical fracture, the surface 'jumps' to its equilibrium position where its hinge moment vanishes. History dependence of aerodynamic loads affects the transient behavior of the surface during the jump and hence affects the amount of mechanical damping that needs to be added to the system in order to avoid catastrophic impact between the surface and its mechanical stop.

*Tel.: +972 (4) 829 3240; fax: +972 (4) 829 2030.
E-mail address: igil@aerodyne.technion.ac.il.

0889-9746/$ - see front matter
doi:10.1016/j.jfluidstructs.2006.09.006

A possible strategy to regain control after actuation failure is to use an electrically or mechanically operated trim tab so as to move the failed surface by changing its aerodynamic hinge moment. This type of control features an inherent time lag between the tab command and the control surface deflection. The amount of lag obviously depends on the inertia of the control surface and on aerodynamic damping and stiffness, but it also depends on the history of the surface motion. Excessive lag increases pilot workload and may lead to pilot-induced oscillations (PIO), and, eventually, to a loss of control (Hodgkinson, 1998). Analysis of the history-dependent effects in both problems is the subject matter of this exposition.

The study of unsteady aerodynamic loads acting on a wing in nonuniform motion has started shortly after the beginning of the last century. The works of Wagner (1925), Glauert (1929), Duncan and Collar (1932), Theodorsen (1935), Küssner (1936), von Karman and Sears (1938), Sears (1940), Söhngen (1939, 1940) and Schwarz (1940) are probably those that set the ground of modern aeroelasticity. All of them addressed a wing section in an unbounded domain of incompressible fluid; works addressing the effects compressibility, finite span, etc. came later. Compilations of theories dealing with unsteady loads can be found in any reference book on aeroelasticity [e.g. Bisplinghoff et al. (1996), Jones (1960), Bisplinghoff and Ashley (1975), Dowell et al. (1989)].

We have found no works on history-dependent effects in relation with control problems considered. Accordingly, we began the present study using the simplest aerodynamic model available. The idea was first to estimate the magnitudes of those effects and the most conspicuous parameters affecting them, and then assess if further refinements will be needed for practical implementation. The simplest of aerodynamic models still accounting for history-dependent effects are those of a wing section in incompressible fluid. Hence any of the works explicitly mentioned above and later works of Jones (1941, 1945), Küssner and Schwarz (1941), and Theodorsen and Garrick (1942), which specifically address wing–aileron–tab-segmented section, could have been used as the aerodynamic basis for the present analysis. Still, we preferred using none of them 'as is'.

Aerodynamic models dealing with unsteady wing motion in incompressible fluid can be classified into two major groups by the way the wing motion is treated. The biggest group encompasses those models where the wing is *a priori* assumed to be executing harmonic motion. The works addressing wing–aileron–tab combinations that were mentioned above belong to this group. A tacit assumption is that the loads acting on an arbitrary moving wing can be obtained from the loads acting on a harmonically oscillating wing using Fourier integrals. The advantage of this approach is in its simplicity; its disadvantage is in the inexistence of Fourier integrals for some of the central cases pertaining to the present study, e.g. an abrupt motion following actuator failure (LePage, 1980, p. 8). The models in this group that do address abrupt motion (as a step) deal with the inexistence of the associated Fourier integrals *ad hoc*, by assuming analytical continuation of the Fourier transforms onto complex (rather than real) frequencies.

In the second group, no *a priori* limiting assumption is made on the way the wing moves, and aerodynamic loads are computed for an arbitrary wing motion using Laplace transforms. Among the few works in this group, the most conspicuous, perhaps, is that of Sears (1940). But with all the appeal of this approach (Edwards, 1979; Edwards et al., 1979), we have not found in this group a direct derivation of aerodynamic loads acting on a generally deforming wing section, and, in particular, on a wing–aileron–tab-segmented one (to be referred later as a 'three-segment wing section'). Accordingly, we took the liberty to repeat, conceptually, the work of Sears (1940), initially extending it to a generally deforming wing section, and then implementing this general result to a three-segment one. The final result was a set of aerodynamic coefficients having simple (short) analytical form which allow obtaining the lift, pitching moment, hinge force and hinge moment acting on a three-segment wing in arbitrary motion.

The aerodynamic part occupies the first eight sections of this manuscript. It is followed by the study of the control surface response to actuator failure and to subsequent deflection of the trim tab.

2. Formulation

Consider an infinitesimally thin wing of infinite aspect ratio moving in a steady uniform flow of incompressible inviscid fluid. Let ρ, U and θ be the density and the velocity of the oncoming fluid and the characteristic time-scale of the wing's undulatory motion, respectively. It is assumed that the amplitude of this motion is small as compared with the wing's semi-chord b, and with the characteristic length-scale $U\theta$ associated with the wing's motion. No restrictions are imposed on the mode of the undulatory motion, and it may involve any combination of torsion, bending, flapping, etc. An infinitesimally thin vortical wake is postulated to exist past the wing, starting at the trailing edge and extending to infinity. To avoid nonlinearity in formulation of the problem, the wake geometrical shape is assumed known *a priori*; specifically, it is assumed that the vorticity is carried from the trailing edge of the wing along straight parallel lines, say, in the direction of the oncoming flow.

It will prove convenient to use dimensionless quantities, with $b, U, b/U, bU, \frac{1}{2}\rho U^2, 2\rho b^2, 2\rho b^4, \rho U^2 b$ and $2\rho U^2 b^2$ serving as units of length, velocity, time, velocity potential, pressure, mass (per unit span), inertia (per unit span), force (per unit span) and moment (per unit span), respectively. Use of dimensionless quantities is implicitly assumed hereafter.

It will also prove convenient to select a right-handed coordinate system, fixed relative to the unmoving wing, with the x-axis lying along the direction of the oncoming flow (and, by assumption, along the direction in which the wake extends), y-axis pointing into the right wing, and z-axis pointing upward. With the origin of the system selected at mid-chord position, the combined wing/wake surface is assumed to be defined by

$$z = f(t, x), \tag{1}$$

where f represents the (known) shape function of that surface, x spans the interval $[-1, \infty)$ and t (time) takes on any value in $(-\infty, \infty)$; the last implication will be tacitly implied hereafter. The magnitude of f and of its first space- and time-derivative is assumed small as compared with unity.

Let μ and p be the potential and pressure jumps across the combined wing/wake surface. These two jumps are formally related by the variant

$$p(t, x) = -2\left(\frac{\partial \mu(t, x)}{\partial t} + \frac{\partial \mu(t, x)}{\partial x}\right) \tag{2}$$

of Bernoulli's theorem, applicable for any x in $(-1, \infty)$. Since no pressure discontinuity can exist across the wake, Eq. (2) infers that μ is carried along the wake with the velocity of the oncoming flow (it equals unity in present notation); thus

$$\mu(t, x) = \mu(t - (x - 1), 1) = \mu_{\mathrm{TE}}(t - x + 1) \tag{3}$$

for each x in $(1, \infty)$. Here, the subscript 'TE' is used to imply the value at the trailing edge. At the leading edge of the wing, continuity of the potential in the immediate vicinity of it necessitates

$$\mu(t, -1) = 0. \tag{4}$$

Using the Biot–Savart law, the impermeability condition at the wing surface can be formulated as

$$\frac{1}{2\pi} \fint_{-1}^{\infty} \frac{\partial \mu(t, x')}{\partial x'} \frac{\mathrm{d}x'}{x - x'} = -\frac{\partial f(t, x)}{\partial t} - \frac{\partial f(t, x)}{\partial x} + \cdots \tag{5}$$

for each x in $(-1,1)$. Here, the bar across the integral sign indicates principal value in Cauchy sense, and the ellipsis stands for terms of higher order with respect to f; these terms will be tacitly neglected in the subsequent derivations. Subject to Eqs. (3) and (4), Eq. (5) furnishes an integro-differential equation for μ. Our first objective is to solve it—once the potential jump is known, the pressure jump across the wing can be computed using Eq. (2); in turn, once the pressure is known, the computation of integral loads (as the hinge moment) presents no conceptual difficulties.

3. Potential jump at the trailing edge

When solving the problem of a moving wing, the right-hand side of Eq. (5) can usually be expressed as a sum of basic 'modes',

$$\frac{\partial f(t, x)}{\partial t} + \frac{\partial f(t, x)}{\partial x} = -\sum_n X_n(x) T_n(t), \tag{6}$$

having shape functions X_1, X_2, etc. and corresponding time dependencies T_1, T_2, etc. Consequently, one can exploit the linearity of Eq. (5), and solve it for a single mode only; general multi-mode solution will be a simple superposition of these single-mode solutions. In the following derivations we shall, therefore, replace Eq. (6) by its singe-mode variant

$$\frac{\partial f(t, x)}{\partial t} + \frac{\partial f(t, x)}{\partial x} = -X(x) T(t); \tag{7}$$

the superposition will be elucidated in Section 7.

Without loss of generality, let us also assume that steady state prevailed prior to time $t = 0$ and that the beginning of the wing motion at $t = 0$ is smooth, implying that all derivatives of T (including T itself) vanish for all $t \leqslant 0$, and

$$\mu(t, x) = \mu_{\mathrm{TE}}(t - x + 1) = 0 \tag{8}$$

for each x in $(t+1,\ \infty)$. Accordingly, with Eqs. (5) and (7),

$$\frac{1}{2\pi}\oint_{-1}^{1}\frac{\partial\mu(t,x')}{\partial x'}\frac{\mathrm{d}x'}{x-x'}=T(t)X(x)+\frac{1}{2\pi}\int_{1}^{1+t}\frac{\mathrm{d}\mu_{\mathrm{TE}}(t-x'+1)}{\mathrm{d}t}\frac{\mathrm{d}x'}{x-x'} \tag{9}$$

for each x in $(-1,1)$. Note the absence of the sum on the right-hand side stemming from our replacing Eq. (6) with Eq. (7). The solution of Eq. (9) will be obtained by loosely following the method of Schwarz (1940), as described in Bisplinghoff et al. (1996, pp. 274–277).

We begin with Söhngen inversion (Söhngen, 1940; Ashley and Landahl, 1985) of Eq. (9); under the assumptions that $\partial\mu/\partial x$ has an integrable singularity at the leading edge and remains finite at the trailing edge (Kutta condition), it yields

$$\begin{aligned}\frac{\partial\mu(t,x)}{\partial x}&=-\frac{2}{\pi}T(t)\sqrt{\frac{1-x}{1+x}}\oint_{-1}^{1}\sqrt{\frac{1+\zeta}{1-\zeta}}\frac{X(\zeta)\mathrm{d}\zeta}{x-\zeta}-\frac{1}{\pi^2}\sqrt{\frac{1-x}{1+x}}\oint_{-1}^{1}\sqrt{\frac{1+\zeta}{1-\zeta}}\frac{\mathrm{d}\zeta}{x-\zeta}\int_{1}^{1+t}\frac{\mathrm{d}\mu_{\mathrm{TE}}(t-x'+1)}{\mathrm{d}t}\frac{\mathrm{d}x'}{\zeta-x'}\\&=-\frac{2}{\pi}T(t)\sqrt{\frac{1-x}{1+x}}\oint_{-1}^{1}\sqrt{\frac{1+\zeta}{1-\zeta}}\frac{X(\zeta)\mathrm{d}\zeta}{x-\zeta}+\frac{1}{\pi}\sqrt{\frac{1-x}{1+x}}\int_{1}^{1+t}\sqrt{\frac{\zeta+1}{\zeta-1}}\frac{\mathrm{d}\mu_{\mathrm{TE}}(t-\zeta+1)}{\mathrm{d}t}\frac{\mathrm{d}\zeta}{x-\zeta}.\end{aligned} \tag{10}$$

Now, using Eq. (4) and (A.1), integration with respect to x between -1 and 1 on both sides of Eq. (10) reduces it to an integro-differential equation,

$$\mu_{\mathrm{TE}}(t)=2T(t)\int_{-1}^{1}\sqrt{\frac{1+x}{1-x}}X(x)\,\mathrm{d}x-\int_{1}^{1+t}\left(\sqrt{\frac{\zeta+1}{\zeta-1}}-1\right)\frac{\mathrm{d}\mu_{\mathrm{TE}}(t-\zeta+1)}{\mathrm{d}t}\,\mathrm{d}\zeta, \tag{11}$$

involving μ_{TE} only. It will be solved first; then μ_{TE} will be substituted back in Eq. (10) to obtain μ; in turn, μ will be substituted back in Eq. (2) to obtain p.

The right-most term in Eq. (11) cancels out with its left hand-side by Eq. (8); upon rearranging the remaining terms, the result can be recast as

$$\int_{1}^{1+t}\sqrt{\frac{\zeta+1}{\zeta-1}}\frac{\mathrm{d}\mu_{\mathrm{TE}}(t-\zeta+1)}{\mathrm{d}t}\,\mathrm{d}\zeta=2T(t)M_0\{X\}, \tag{12}$$

where $M_0\{\ldots\}$ denotes the operator

$$M_0\{X\}=\int_{-1}^{1}\sqrt{\frac{1+x}{1-x}}X(x)\,\mathrm{d}x. \tag{13}$$

The use of the subscript '0' with M is made to fit subsequent notation. An alternative, and perhaps more convenient, variant of Eq. (12),

$$\int_{0}^{t}\sqrt{\frac{\eta+2}{\eta}}\frac{\mathrm{d}\mu_{\mathrm{TE}}(t-\eta)}{\mathrm{d}t}\,\mathrm{d}\eta=2T(t)M_0\{X\}, \tag{14}$$

can be readily obtained from the former by changing the integration variable to $\eta=\zeta-1$.

Solution of Eq. (14) is straightforward. Starting with the Laplace transform [see, for example, LePage (1980, p. 298)],

$$L\{\ldots;s\}=\int_{0}^{\infty}\ldots(t)\mathrm{e}^{-st}\mathrm{d}t, \tag{15}$$

on both sides, and using convolution theorem (see, for example, p. 343 ibid.) on the left-hand side, one should find no difficulty to obtain

$$s\mathrm{e}^{s}(\mathrm{K}_0(s)+\mathrm{K}_1(s))L\{\mu_{\mathrm{TE}};s\}=2M_0\{X\}L\{T;s\}, \tag{16}$$

where K_0 and K_1 are the respective Bessel functions of an imaginary argument; the associated integrals can be found in Gradshteyn and Ryzhik (1980, Art. 3.372). Equivalently,

$$L\{\mu_{\mathrm{TE}};s\}=2M_0\{X\}\hat{G}_n(s)s^nL\{T;s\}, \tag{17}$$

where n is any integer, and $\hat{G}_n$ is an auxiliary function defined by

$$\hat{G}_n(s)=\frac{\mathrm{e}^{-s}}{s^{n+1}}\frac{1}{\mathrm{K}_0(s)+\mathrm{K}_1(s)}. \tag{18}$$

The solution of Eq. (14) now immediately follows Eq. (17) by definition of the inverse transform [see, for example, LePage, (1980, p. 319)],

$$L^{-1}\{\ldots;t\}=\frac{1}{2\pi\mathrm{i}}\int_{\gamma-\mathrm{i}\infty}^{\gamma+\mathrm{i}\infty}\ldots(s)\mathrm{e}^{st}\,\mathrm{d}s; \tag{19}$$

it can be written as any of the convolutions

$$\mu_{\mathrm{TE}}(t)=2M_0\{X\}\int_0^t G_n(t-\tau)\frac{\mathrm{d}^nT(\tau)}{\mathrm{d}\tau^n}\,\mathrm{d}\tau \tag{20}$$

of the nth derivative of T with standard functions

$$G_n(t)=L^{-1}\{\hat{G}_n;t\}. \tag{21}$$

In Eq. (19) γ is a real constant exceeding the real part of the all singularities of the integrand; the respective integration path is often referred to as the Bromwich contour—see pp. 319–320 ibid.

By interpretation, the functions G_0, G_1, G_2, etc. represent the trailing-edge potential jump (or, else, the circulation around the wing) responses to a unit impulse, step, ramp, etc.; the function G_1 will be identified later with the Küssner's function for lift due to sharp-edged gust (Sears, 1940). The subscript n of G in Eqs. (17), (18), (20) and (21), representing the order of the derivative of T with which G_n convolves in Eq. (20) to yield μ_{TE}, will be referred to as the order of the standard response. By this definition, unit impulse response is of order zero, step response is of order unity, etc.

$\hat{G}_n(s)$ behaves as s^{-n} for small s, and as $(2\pi s^{2n+1})^{-1/2}$ for large s. The former limit implies that all standard responses of order $n\geqslant 2$ diverge when t goes to infinity (cf. the final-value theorem); the latter limits implies that for short times,

$$G_n(t)=\frac{t^n}{\sqrt{2\pi t}}\frac{1}{\Gamma(n+\frac{1}{2})}+\cdots=\frac{(2t)^{n-1/2}}{\pi(2n-1)!!}+\cdots, \tag{22}$$

and hence all standard responses of order $n\leqslant 0$ diverge when t goes to zero. It leaves the case $n=1$ (step) as the only one for which the standard response remains finite at all times. Functions G_0 and G_1 are shown in Fig. 1; the singular part of G_0, $(\pi\sqrt{2t})^{-1}$, has been subtracted from the respective function shown on the left.

4. Pressure jump

Once μ_{TE} has been found, we proceed with the computation of p, which requires knowledge of the two partial derivatives of μ—see Eq. (2). The derivative $\partial\mu/\partial x$ is readily given by Eq. (10). In order to find $\partial\mu/\partial t$ we suggest first differentiating $\partial\mu/\partial x$ with respect to time, and then integrating the result with respect to x. Noting the initial conditions (zero), the first step yields

$$\frac{\partial^2\mu(t,x)}{\partial t\partial x}=-\frac{2}{\pi}\frac{\mathrm{d}T(t)}{\mathrm{d}t}\sqrt{\frac{1-x}{1+x}}\fint_{-1}^{1}\sqrt{\frac{1+\zeta}{1-\zeta}}\frac{X(\zeta)\mathrm{d}\zeta}{x-\zeta}+\frac{1}{\pi}\sqrt{\frac{1-x}{1+x}}\int_1^{1+t}\sqrt{\frac{\zeta+1}{\zeta-1}}\frac{\mathrm{d}^2\mu_{\mathrm{TE}}(t-\zeta+1)}{\mathrm{d}t^2}\frac{\mathrm{d}\zeta}{x-\zeta}. \tag{23}$$

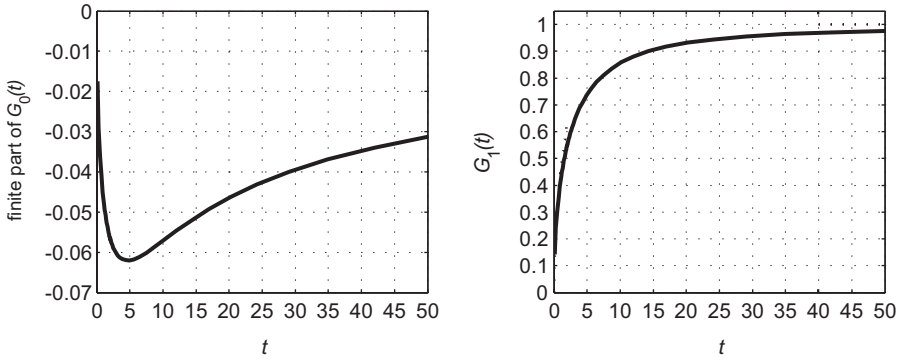

Fig. 1. Functions $t\to G_0(t)-(\pi\sqrt{2t})^{-1}$ and G_1; dotted lines on the right figure mark the respective asymptotic limits.

The integration with respect to x is somewhat tedious. Still, using Eq. (4), as well as Eqs. (A.3) and (A.4) from Appendix A, one should find no difficulty to obtain

$$\frac{\partial\mu(t,x)}{\partial t} = -\frac{2}{\pi}(\cos^{-1}x-\pi)\frac{\mathrm{d}T(t)}{\mathrm{d}t}\int_{-1}^{1}\sqrt{\frac{1+\zeta}{1-\zeta}}X(\zeta)\mathrm{d}\zeta+\frac{2}{\pi}\frac{\mathrm{d}T(t)}{\mathrm{d}t}\int_{-1}^{1}\Lambda_1(x,\zeta)X(\zeta)\,\mathrm{d}\zeta$$
$$+\frac{1}{\pi}(\cos^{-1}x-\pi)\int_{1}^{1+t}\left(\sqrt{\frac{\zeta+1}{\zeta-1}}-1\right)\frac{\mathrm{d}^2\mu_{\mathrm{TE}}(t-\zeta+1)}{\mathrm{d}t^2}\,\mathrm{d}\zeta-\frac{2}{\pi}\int_{1}^{1+t}\Lambda_2(x,\zeta)\frac{\mathrm{d}^2\mu_{\mathrm{TE}}(t-\zeta+1)}{\mathrm{d}t^2}\,\mathrm{d}\zeta, \quad (24)$$

where

$$\Lambda_1(x,\zeta)=\ln\left|\frac{\sqrt{(1-x)(1+\zeta)}+\sqrt{(1+x)(1-\zeta)}}{\sqrt{(1-x)(1+\zeta)}-\sqrt{(1+x)(1-\zeta)}}\right| \quad (25)$$

and

$$\Lambda_2(x,\zeta)=\tan^{-1}\sqrt{\frac{(\zeta+1)(1-x)}{(\zeta-1)(1+x)}}-\frac{\cos^{-1}x}{2}. \quad (26)$$

The last step toward simplification of Eq. (24) before its substitution back in Eq. (2) involves integration by parts in its right-most term; using Eqs. (11) and (8) to nullify the combination of the first, the third, and one of the terms arising during the integration by parts, the result can be recast as

$$\frac{\partial\mu(t,x)}{\partial t}=\frac{2}{\pi}\frac{\mathrm{d}T(t)}{\mathrm{d}t}\int_{-1}^{1}\Lambda_1(x,\zeta)X(\zeta)\mathrm{d}\zeta+\frac{1}{\pi}\int_{1}^{1+t}\sqrt{\frac{1-x^2}{\zeta^2-1}}\frac{\mathrm{d}\mu_{\mathrm{TE}}(t-\zeta+1)}{\mathrm{d}t}\frac{\mathrm{d}\zeta}{\zeta-x}. \quad (27)$$

Hence,

$$p(t,x)=\frac{4}{\pi}T(t)\sqrt{\frac{1-x}{1+x}}\int_{-1}^{1}\sqrt{\frac{1+\zeta}{1-\zeta}}\frac{X(\zeta)\mathrm{d}\zeta}{x-\zeta}-\frac{4}{\pi}\frac{\mathrm{d}T(t)}{\mathrm{d}t}\int_{-1}^{1}\Lambda_1(x,\zeta)X(\zeta)\,\mathrm{d}\zeta$$
$$+\frac{2}{\pi}\sqrt{\frac{1-x}{1+x}}\int_{1}^{1+t}\frac{\mathrm{d}\mu_{\mathrm{TE}}(t-\zeta+1)}{\mathrm{d}t}\frac{\mathrm{d}\zeta}{\sqrt{\zeta^2-1}}, \quad (28)$$

by Eqs. (10) and (2).

The integral on the right-most of Eq. (28),

$$\int_{1}^{1+t}\frac{\mathrm{d}\mu_{\mathrm{TE}}(t-\zeta+1)}{\mathrm{d}t}\frac{\mathrm{d}\zeta}{\sqrt{\zeta^2-1}}=\int_{0}^{t}\frac{\mathrm{d}\mu_{\mathrm{TE}}(t-\xi)}{\mathrm{d}t}\frac{\mathrm{d}\xi}{\sqrt{\xi(\xi+2)}}, \quad (29)$$

can be identified as a convolution of $\mathrm{d}\mu_{\mathrm{TE}}/\mathrm{d}t$ with the function $t\to\left[\sqrt{t(t+2)}\right]^{-1}$, and therefore it can be interpreted as the inverse transform of the product of respective Laplace transforms. Both are known: the transform of $\mathrm{d}\mu_{\mathrm{TE}}/\mathrm{d}t$ given by Eq. (17), and the transform of $t\to\left[\sqrt{t(t+2)}\right]^{-1}$ equals $\mathrm{e}^{s}\mathrm{K}_0(s)$ [see Gradshteyn and Ryzhik (1980, Art. 3.264.3)]; accordingly,

$$p(t,x)=\frac{4}{\pi}T(t)\sqrt{\frac{1-x}{1+x}}\int_{-1}^{1}\sqrt{\frac{1+\zeta}{1-\zeta}}\frac{X(\zeta)\mathrm{d}\zeta}{x-\zeta}-\frac{4}{\pi}\frac{\mathrm{d}T(t)}{\mathrm{d}t}\int_{-1}^{1}\Lambda_1(x,\zeta)X(\zeta)\mathrm{d}\zeta+\frac{4}{\pi}W\{T;t\}M_0\{X\}\sqrt{\frac{1-x}{1+x}}, \quad (30)$$

where

$$W\{T;t\}=L^{-1}\{s\to(\hat{G}_n(s)s^{n+1}L\{T;s\})\ (\mathrm{e}^{s}\mathrm{K}_0(s));\ \ t\}. \quad (31)$$

But then, using the convolution theorem, the inverse transform on the right-hand side of Eq. (31) can be recast as any of the convolutions,

$$W\{T;t\}=\int_{0}^{t}P_n(t-\tau)\frac{\mathrm{d}^nT(\tau)}{\mathrm{d}\tau^n}\,\mathrm{d}\tau, \quad (32)$$

of the nth derivative of T, the inverse transform of $s\to s^nL\{T;s\}$, with

$$P_n(t)=L^{-1}\{\hat{P}_n;t\}, \quad (33)$$

the inverse transform of

$$\hat{P}_n(s) = se^s \hat{G}_n(s)\mathrm{K}_0(s) = \frac{1}{s^n}\frac{\mathrm{K}_0(s)}{\mathrm{K}_0(s)+\mathrm{K}_1(s)}. \tag{34}$$

By interpretation, P_0, P_1, P_2, etc. represent standard partial responses of the pressure jump across the wing surface to a unit impulse, step, ramp, etc.; full responses to these inputs obviously involve the first two terms on the right-hand side of Eq. (30) as well.

It immediately follows from Eq. (34) that $\hat{P}_n$ behaves as

$$\hat{P}_n(s) = s^{1-n}(\ln 2 - \ln s - \gamma) - s^{2-n}(\ln 2 - \ln s - \gamma)^2 + \ldots \tag{35}$$

for small s (here, $\gamma = 0.5772\ldots$ is the Euler constant), and as

$$\hat{P}_n(s) = \frac{1}{2s^n} - \frac{1}{8s^{n+1}} + \frac{1}{16s^{n+2}} + \ldots \tag{36}$$

for large s. Accordingly, $P_0(t)$ vanishes when t goes to infinity (cf. the final value theorem), and behaves as a combination

$$P_0(t) = \frac{1}{2}\delta(t) - \frac{1}{8}\mathscr{H}(t) + \frac{1}{16}t + \ldots \tag{37}$$

of Dirac delta (δ) and Heaviside step ($\mathscr{H}$) functions for small t; the delta function contribution has been removed from the function shown in Fig. 2. $P_1(t)$ also vanishes when t goes to infinity, but remains finite for small t, behaving as

$$P_1(t) = \frac{1}{2}\mathscr{H}(t) - \frac{1}{8}t + \ldots; \tag{38}$$

it was shown unaltered in Fig. 2. All higher-order functions diverge when t goes to infinity, but vanish when t goes to zero. This leaves the step response ($n = 1$) as the only one remaining finite at all times: lower-order responses ($n<1$) diverge at short times; higher-order ($n>1$) diverge at long times. The combination $t \to \mathscr{H}(t) - P_1(t)$ of the step response will be identified later with the Wagner's function (Sears, 1940).

5. Forces and moments

The normal force and the moment about the point $x = h$ created by a segment $(a, 1)$ of the wing are given by

$$F(t,a) = -\frac{1}{2}\int_a^1 p(t,x)\,\mathrm{d}x \tag{39}$$

and

$$M(t,a,h) = \frac{1}{4}\int_a^1 (x-h)p(t,x)\,\mathrm{d}x, \tag{40}$$

respectively. Particular cases of Eqs. (39) and (40) are the lift and mid-chord pitching moment (h equals 0) of the entire wing (a equals -1), and the force and moment acting on the hinge (a equals h and equals hinge position from the

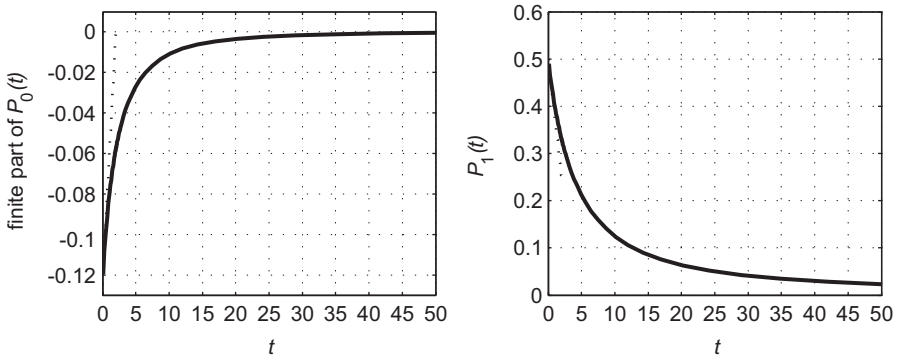

Fig. 2. Functions $t \to P_0(t) - \frac{1}{2}\delta(t)$ and P_1; asymptotic limits are shown by broken lines.

mid-chord). Note that the units of force and moment, $\rho U^2 b$ and $2\rho U^2 b^2$, used in Eqs. (39) and (40) are standard considering the force and moment acting on the entire wing section; they are not standard considering the force and moment acting on the hinge. For example, standard units used in flight mechanics are $\frac{1}{2}(1-h)$ and $\frac{1}{4}(1-h)^2$ times those used herein—see, for example, Etkin and Reid (1996). It is hoped that no confusion will result.

It is always possible to express the moment $M(t,a,h)$ about the point $x=h$ in terms of the moment $M(t,a,0)$ about the mid-chord and the force $F(t,a)$; in fact,

$$M(t,a,h) = M(t,a,0) + \frac{h}{2}F(t,a), \tag{41}$$

by definition. Accordingly, without loss of generality, we shall proceed addressing the last two quantities only.

With Eq. (30), Eqs. (39) and (40) can be recast as

$$F(t,a) = Q_T^{(0)}\{X;a\}T(t) + Q_{\dot{T}}^{(0)}\{X;a\}\frac{\mathrm{d}T(t)}{\mathrm{d}t} + Q_{\widehat{T}}^{(0)}\{X;a\}W\{T;t\}, \tag{42}$$

$$M(t,a,0) = Q_T^{(1)}\{X;a\}T(t) + Q_{\dot{T}}^{(1)}\{X;a\}\frac{\mathrm{d}T(t)}{\mathrm{d}t} + Q_{\widehat{T}}^{(1)}\{X;a\}W\{T;t\}, \tag{43}$$

where W is the operator defined in Eq. (32), and Q's are integral operators

$$Q_T^{(n)}\{X;a\} = \frac{(-2)^{1-n}}{\pi}\int_{-1}^{1}\sqrt{\frac{1+\zeta}{1-\zeta}}X(\zeta)\mathrm{d}\zeta\oint_a^1\sqrt{\frac{1-x}{1+x}}\frac{x^n\,\mathrm{d}x}{x-\zeta}, \tag{44}$$

$$Q_{\dot{T}}^{(n)}\{X;a\} = -\frac{(-2)^{1-n}}{\pi}\int_{-1}^{1}X(\zeta)\mathrm{d}\zeta\oint_{-1}^{1}\Lambda_1(x,\zeta)x^n\,\mathrm{d}x, \tag{45}$$

$$Q_{\widehat{T}}^{(n)}\{X;a\} = \frac{(-2)^{1-n}}{\pi}\int_{-1}^{1}\sqrt{\frac{1+\zeta}{1-\zeta}}X(\zeta)\mathrm{d}\zeta\int_a^1\sqrt{\frac{1-x}{1+x}}x^n\mathrm{d}x. \tag{46}$$

For the sake of symmetry, we have explicated $M_0\{X\}$, otherwise appearing in Eq. (46), using its definition (13).

Each of the respective inner integrals in Eqs. (44)–(46), those with respect to x, can be computed analytically and is listed at the beginning of Appendix A —cf. Eqs. (A.5)–(A.10) thereat. In turn, the remaining integrals, those with respect to ζ, can be expressed as linear combinations of six primitive integrals,

$$M_n\{X\} = \int_{-1}^{1}\sqrt{\frac{1+\zeta}{1-\zeta}}X(\zeta)(1-\zeta)^n\,\mathrm{d}\zeta, \tag{47}$$

$$N_n\{X;a\} = \oint_{-1}^{1}X(\zeta)(\zeta-a)^n\Lambda_1(a,\zeta)\mathrm{d}\zeta, \tag{48}$$

(n equals 0, 1 or 2), which can be computed once the shape function X of the respective wing motion is known ($n=0$ variant of Eq. (47) has been already defined in Eq. (13)—hence the subscript '0' that was used thereat). The resulting expressions become

$$Q_T^{(0)}\{X;a\} = \frac{2}{\pi}(M_0\{X\}\cos^{-1}a - N_0\{X;a\}), \tag{49}$$

$$Q_{\dot{T}}^{(0)}\{X;a\} = \frac{2}{\pi}(M_1\{X\}\cos^{-1}a + N_1\{X;a\}), \tag{50}$$

$$Q_{\widehat{T}}^{(0)}\{X;a\} = -\frac{2}{\pi}(\cos^{-1}a - \sqrt{1-a^2})M_0\{X\}, \tag{51}$$

$$Q_T^{(1)}\{X;a\} = \frac{1}{\pi}(M_1\{X\}\cos^{-1}a + N_1\{X;a\} - M_0\{X\}\sqrt{1-a^2} + aN_0\{X;a\}), \tag{52}$$

$$Q_{\dot{T}}^{(1)}\{X;a\} = \frac{1}{2\pi}\Big((M_2\{X\} - M_1\{X\})\cos^{-1}a - M_1\{X\}\sqrt{1-a^2} - N_2\{X;a\} - 2aN_1\{X;a\}\Big), \tag{53}$$

$$Q_{\widehat{T}}^{(1)}\{X;a\} = -\frac{1}{2\pi}(\cos^{-1}a - (2-a)\sqrt{1-a^2})M_0\{X\}. \tag{54}$$

The lift and the mid-chord-moment acting on the entire wing can be obtained from the above by setting $a=-1$. This makes all the Ns and the square roots in Eqs. (49)–(54) vanish; whereas substitution of what has been left back in Eqs. (42) and (43) yields

$$F(t,-1)=2M_0\{X\}(T(t)-W\{T;t\})+2M_1\{X\}\frac{\mathrm{d}T(t)}{\mathrm{d}t}, \tag{55}$$

$$M(t,-1,0)=M_1\{X\}T(t)-\frac{1}{2}M_0\{X\}W\{T;t\}+\frac{1}{2}(M_2\{X\}-M_1\{X\})\frac{\mathrm{d}T(t)}{\mathrm{d}t}. \tag{56}$$

For future reference we note that the moment

$$M\big(t,-1,-1/2\big)=M(t,-1,0)-\frac{1}{4}F(t,-1)=\left(M_1\{X\}-\frac{1}{2}M_0\{X\}\right)T(t)+\left(\frac{1}{2}M_2\{X\}-M_1\{X\}\right)\frac{\mathrm{d}T(t)}{\mathrm{d}t} \tag{57}$$

about the quarter chord point—cf. Eq. (41)—is independent of the history of the wing's motion. Indeed, all aerodynamic loads induced by the wake on a harmonically oscillating wing section are known to act at the quarter-chord point—see Bisplinghoff et al. (1996, p. 278); Eq. (57) is a direct generalization for an arbitrary motion.

6. Particular cases

6.1. Steady state solution

For future reference, as well as for comparison with known results, consider aerodynamic forces acting on the wing section a long time ($t\to\infty$) after the step $T(t)=\mathscr{H}(t)$ has been introduced. In this case, $W\{T;t\}=P_1(t)$ and hence vanishes as $t\to\infty$—see the discussion following Eq (37). Accordingly,

$$\lim_{t\to\infty}F(t,a)=Q_T^{(0)}\{X;a\}=\frac{2}{\pi}(M_0\{X\}\cos^{-1}a-N_0\{X;a\}), \tag{58}$$

$$\lim_{t\to\infty}M(t,a,0)=Q_T^{(1)}\{X;a\}=\frac{1}{\pi}(M_1\{X\}\cos^{-1}a+N_1\{X;a\}-M_0\{X\}\sqrt{1-a^2}+aN_0\{X;a\}). \tag{59}$$

A particular case of Eqs. (58) and (59) concerns the forces acting on the entire wing; since N_0 and N_1 vanish when $a=-1$,

$$\lim_{t\to\infty}F(t,-1)=2M_0\{X\}, \tag{60}$$

$$\lim_{t\to\infty}M(t,-1,0)=M_1\{X\}. \tag{61}$$

Both results are, of course, well known, albeit in somewhat different notation—see, for example, Bisplinghoff and Ashley (1975, p. 86).

6.2. Oscillating wing

Another case for comparison with known solutions is the case where the wing executes harmonic oscillations with $T(t)=\mathrm{e}^{\mathrm{i}kt}$ since a long-long time ($t\to\infty$). Under these circumstances, the history-dependent term becomes

$$\lim_{t\to\infty}W\{T;t\}=\lim_{t\to\infty}\int_0^t P_0(t-\tau)\mathrm{e}^{\mathrm{i}k\tau}\,\mathrm{d}\tau=\mathrm{e}^{\mathrm{i}kt}\lim_{t\to\infty}\int_0^t P_0(t-\tau)\mathrm{e}^{-\mathrm{i}k(t-\tau)}\,\mathrm{d}\tau=\mathrm{e}^{\mathrm{i}kt}\int_0^\infty P_0(\xi)\mathrm{e}^{-\mathrm{i}k\xi}\,\mathrm{d}\xi. \tag{62}$$

The integral on the right will be readily identified with $\hat{P}_0(\mathrm{i}k)=L\{P_0;\mathrm{i}k\}$, and therefore

$$\lim_{t\to\infty}W\{T;t\}=\hat{P}_0(\mathrm{i}k)\mathrm{e}^{\mathrm{i}kt}=\frac{\mathrm{K}_0(\mathrm{i}k)\mathrm{e}^{\mathrm{i}kt}}{\mathrm{K}_0(\mathrm{i}k)+\mathrm{K}_1(\mathrm{i}k)}, \tag{63}$$

by Eq. (34). Noting the relation $\mathrm{K}_n(\mathrm{i}k)=-(\mathrm{i}\pi/2)\exp(-\mathrm{i}\pi n/2)\mathrm{H}_n^{(2)}(k)$ between the respective Bessel functions—see Gradshteyn and Ryzhik (1980, Arts. 8.407.1 and 8.476.8)—Eq (63) can be rewritten in an equivalent form

$$\lim_{t\to\infty}W\{T;t\}=\frac{\mathrm{i}\mathrm{H}_0^{(2)}(k)\mathrm{e}^{\mathrm{i}kt}}{\mathrm{H}_1^{(2)}(k)+\mathrm{i}\mathrm{H}_0^{(2)}(k)}=(1-C(k))\mathrm{e}^{\mathrm{i}kt}, \tag{64}$$

where C stands for the standard combination of Hankel functions,

$$C(k)=\frac{\mathrm{H}_1^{(2)}(k)}{\mathrm{H}_1^{(2)}(k)+\mathrm{i}\mathrm{H}_0^{(2)}(k)}, \tag{65}$$

commonly known as 'Theodorsen's lift deficiency function'.

The conjunction of Eq. (55), (56) and (64) now recovers the well-known results:

$$F(t,-1)=2\mathrm{e}^{\mathrm{i}kt}(\mathrm{i}kM_1\{X\}+M_0\{X\}C(k)), \tag{66}$$

$$M(t,-1,0)=\frac{\mathrm{e}^{\mathrm{i}kt}}{2}\left((2M_1\{X\}-M_0\{X\})+\mathrm{i}k(M_2\{X\}-M_1\{X\})+M_0\{X\}C(k)\right); \tag{67}$$

for the first of these the reader is referred to Ashley and Landahl (1985, p. 255).

6.3. Wagner's function

Yet another case for comparison with known solutions is the case where the time function is a step, i.e. $T(t)=\mathscr{H}(t)$. In this case,

$$W\{\mathscr{H};t\}=P_1(t), \tag{68}$$

by definition (32); consequently,

$$F(t,-1)=2M_0\{X\}(\mathscr{H}(t)-P_1(t))+2M_1\{X\}\delta(t), \tag{69}$$

by Eq. (55). Noting that

$$L\{\mathscr{H};s\}-L\{P_1;s\}=\frac{1}{s}\frac{\mathrm{K}_1(s)}{\mathrm{K}_1(s)+\mathrm{K}_0(s)} \tag{70}$$

by Eq. (34), the function $t\to\mathscr{H}(t)-P_1(t)$, appearing on the right-hand side of Eq. (69), will be readily identified with the Wagner's function—see Bisplinghoff et al. (1996, pp. 284–285).

6.4. Küssner's function

The problem of aerodynamic loads on a wing flying through stationary (i.e. time independent as viewed from a stationary reference frame) vertical gust of velocity v is not directly related with the problem of controlling the aircraft with trim tabs. Still, under the same assumptions, the only difference between the gust problem and that solved hereinabove is in impermeability condition, where

$$\frac{1}{2\pi}\fint_{-1}^{\infty}\frac{\partial\mu(t,x')}{\partial x'}\frac{\mathrm{d}x'}{x-x'}=v(t-x-1) \tag{71}$$

replaces Eq. (5) as the one to be satisfied for each x in $(-1, 1)$. This similarity allows obtaining all aerodynamic loads by merely repeating the same steps as those leading to Eqs. (20), (30), (42) and (43) with $v(t-x-1)$ instead of $X(x)T(t)$. With details found in Appendix B, the results are

$$p(t,x)=-4\sqrt{\frac{1-x}{1+x}}\int_0^t G_n(t-\tau)\frac{\mathrm{d}^n v(\tau)}{\mathrm{d}\tau^n}\,\mathrm{d}\tau, \tag{72}$$

$$F(t,a)=2(\cos^{-1}a-\sqrt{1-a^2})\int_0^t G_n(t-\tau)\frac{\mathrm{d}^n v(\tau)}{\mathrm{d}\tau^n}\mathrm{d}\tau, \tag{73}$$

$$M(t,a,h)=F(t,a)\left(\frac{2h+1}{4}-\frac{(1-a)\sqrt{1-a^2}}{4(\cos^{-1}a-\sqrt{1-a^2})}\right). \tag{74}$$

It immediately follows that the functions G_0, G_1, etc., previously associated with standard circulation responses to impulse, step, etc. in the normal-to-the-wing velocity component, also represent standard aerodynamic load responses to impulse, step, etc. in the gust velocity. In particular, with $v(t)=\mathscr{H}(t)$,

$$F(t,-1)=2\pi G_1(t), \tag{75}$$

$$M(t,-1,-1/2)=0. \tag{76}$$

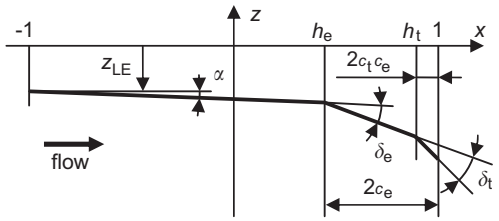

Fig. 3. Three-segment wing section.

The former identifies G_1 with Küssner's function—cf. Sears (1940); the latter supports Eq. (57) by obtaining the quarter-chord moment independent of the gust characteristics. Sixty-five years after Sears, we still can offer no physical explanation why circulation response to a step in the normal-to-the wing velocity should mimic the pressure response to a sharp-edged gust.

7. Three-segment wing section

Consider now the case where the wing section consists of three rigid segments, connected by means of two hinges, as shown in Fig. 3. The rearmost segment represents the trim tab; the conjunction of the two rearmost segments represents the primary control surface—e.g. aileron, rudder or elevator. The ratio of the control surface chord (the length of the two rearmost segments together) to the section chord (the length of all wing segments together) will be denoted as c_e; the ratio of the tab chord (length of the rearmost segment) to the control surface chord will be denoted as c_t.

For the three-segment wing, the right-hand side of Eq. (1) takes on the form

$$f(t,x) = f_0(x) - \sum_{n=1}^{4} f_n(x) q_n(t), \tag{77}$$

where f_0 describes the mean-camber-line, and the remaining functions are summarized in Table 1. Of these, $q_1 = z_{LE}$ is vertical (positive down) coordinate of the leading-edge; $q_2 = \alpha$ is the angle of attack; $q_3 = \delta_e$ and $q_4 = \delta_t$ are the deflection angles of the control surface and the tab, respectively (positive for trailing edge down);

$$h_e = 1 - 2c_e \text{ and } h_t = 1 - 2c_e c_t \tag{78}$$

are the coordinates of the respective hinges; and angular brackets are used to imply

$$\langle \dots \rangle^n = (\dots)^n \mathscr{H}(\dots) \tag{79}$$

for any nonnegative n.

With Eq. (77), the right-hand side of Eq. (6) becomes a superposition of nine different 'modes', each identified by a unique product of time-dependent ($q_1,\dots, q_4$ and their first derivatives) and coordinate-dependent ($f_1,\dots, f_4$ and their first derivatives) functions. Specifically, with an over-dot denoting a derivative of the respective function,[1]

$$X_0(x) = -\dot{f}_0(x), \quad T_0(t) = 1, \tag{80}$$

whereas for each $n = 1,\dots,4$,

$$X_n(x) = \dot{f}_n(x), \quad T_n(t) = q_n(t), \quad X_{n+4}(x) = f_n(x), \quad T_{n+4}(t) = \dot{q}_n(t). \tag{81}$$

Accordingly, with Eq. (41) remaining unchanged, Eqs. (42) and (43) become

$$\begin{aligned} F(t,a) = & -Q_T^{(0)}\{\dot{f}_0;a\} + \sum_{n=1}^{4}\Big(Q_{\dot{T}}^{(0)}\{f_n;a\}\ddot{q}_n(t) + (Q_{\dot{T}}^{(0)}\{\dot{f}_n;a\} + Q_T^{(0)}\{f_n;a\})\dot{q}_n(t) \\ & + Q_T^{(0)}\{\dot{f}_n;a\}q_n(t) + Q_{\widehat{T}}^{(0)}\{f_n;a\}W\{\dot{q}_n;t\} + Q_{\widehat{T}}^{(0)}\{\dot{f}_n;a\}W\{q_n;t\}\Big), \end{aligned} \tag{82}$$

[1]The time-dependent function of this 'mode' does not comply with the assumption that T is zero for all times prior to zero. Formal solution corresponding to this case can be obtained from the above formulae by setting $T(t) = \mathscr{H}(t)$ and taking t to infinity (see Section 6.1). Practically, however, it is equivalent with setting $T = 1$ directly.

Table 1
The shape functions and degrees of freedom of the three-segment wing

n	1	2	3	4
f_n	1	$x+1$	$\langle x-h_e\rangle$	$\langle x-h_t\rangle$
q_n	z_{LE}	α	δ_e	δ_t

$$M(t,a,0) = -Q_T^{(1)}\{\dot f_0;a\} + \sum_{n=1}^{4}\Big(Q_{\dot T}^{(1)}\{f_n;a\}\ddot q_n(t) + (Q_{\dot T}^{(1)}\{\dot f_n;a\} + Q_T^{(1)}\{f_n;a\})\dot q_n(t) + Q_T^{(1)}\{\dot f_n;a\}q_n(t) + Q_{\widetilde T}^{(1)}\{f_n;a\}W\{\dot q_n;t\} + Q_{\widehat T}^{(1)}\{\dot f_n;a\}W\{q_n;t\}\Big). \tag{83}$$

Here, the Qs appearing first on the right-hand sides of these two equations are initial steady-state force and couple acting on the pertinent part of the section; they may be computed once the function f_0 describing the mean camber-line of the wing is known. At the same time, all other Qs can be (and have been) computed analytically using the integrals listed in Appendix A. The results are concentrated in Appendix C.

Eqs. (82) and (83) infer that any integral aerodynamic load Λ, and, in particular, the lift $F(t,-1)$, the mid-chord pitching moment $M(t,-1,0)$, the quarter-chord pitching moment $M(t,-1,-1/2)$, the hinge force $F(t,h_e)$ and the hinge moment $M(t,h_e,h_e)$, can be expressed symbolically as

$$\Lambda(t) = \Lambda_0 + \sum_{n=1}^{4}(A_n\ddot q_n(t) + B_n\dot q_n(t) + C_n q_n(t) + D_n W\{\dot q_n;t\} + E_n W\{q_n;t\}), \tag{84}$$

where load-specific coefficients $\Lambda_0 = \Lambda(-0)$ and $A_1,\dots,E_4$ can be easily identified with the particular combinations of Q's (see Table 2), and hence possess closed analytical forms. Being both lengthy and obvious, we shall not explicate them here. For the case of harmonic oscillations—when W is given by Eq. (64)—they can be identified with pertinent combinations of T and Y-integrals of Theodorsen and Garrick (1942) or X and $\bar X$-integrals of Jones (1941). Simplified versions of these expressions, representing only the first one or two terms in their respective asymptotic series with respect to c_e and c_t, are listed in Table 3.

Coefficients $A_1,\dots,E_4$ for the lift, mid- and quarter-chord pitching moments and hinge force and moment are shown in Figs. 4–8 together with asymptotic approximations of Table 3. The quality of these approximations seems to be very fair for the entire range of c_e and c_t shown. In fact, it is fair enough to express the coefficients $A_1,\dots,E_4$ as respective products of certain (reduced) coefficients, $a_1,\dots,e_4$, only weakly (if at all) dependent upon the dimensions of the control surface and the tab, and powers of c_e and c_t. With these, Eq. (84) can be recast as

$$\begin{aligned}\Lambda(t)-\Lambda_0 = {}& (-1)^l c_e^{n/2}(a_1\ddot z_{LE} + b_1\dot z_{LE} + c_1 z_{LE} - (d_1 W\{\dot z_{LE};t\} + e_1 W\{z_{LE};t\}))\\ &+ (-1)^l c_e^{n/2}(a_2\ddot\alpha + b_2\dot\alpha + c_2\alpha - (d_2 W\{\dot\alpha;t\} + e_2 W\{\alpha;t\}))\\ &+ (-1)^l c_e^{(n+m)/2}(a_3 c_e^2\ddot\delta_e + b_3 c_e\dot\delta_e + c_3\delta_e - c_e^k(d_3 c_e W\{\dot\delta_e;t\} + e_3 W\{\delta_e;t\}))\\ &+ (-1)^l c_e^{(n+m)/2}c_t^{1/2}(a_4 c_e^2 c_t^2\ddot\delta_t + b_4 c_e c_t\dot\delta_t + c_4\delta_t - c_e^k(d_4 c_e c_t W\{\dot\delta_t;t\} + e_4 W\{\delta_t;t\})),\end{aligned} \tag{85}$$

where (load-specific) powers l, m and n are listed in Table 4. Approximations for (load-specific) coefficients $a_1,\dots,e_4$ immediately follow those of Table 3 and hence will not be repeated here; toward the discussion of the following sections it is material that these coefficients are all nonnegative and of comparable magnitudes.

8. History-dependent effects

It appears that any integral aerodynamic load on a wing (or part of it) can be naturally sub-divided into instantaneous and history-dependent constituents. The former depends on the (generalized) displacements, rates and accelerations and governed by the coefficients $a_1,\dots,a_4$, $b_1,\dots,b_4$ and $c_1,\dots,c_4$. The latter depends on the convolutions W of the displacements and rates with P_0 (or rates and accelerations with P_1, or accelerations and jerks with P_2, etc.) and governed by the coefficients $d_1,\dots,d_4$ and $e_1,\dots,e_4$. History-dependent constituents of the hinge

Table 2
Coefficients in Eq. (84); $a=-1$ for the loads acting on the entire wing; $a=h_e$ for the loads acting on the surface only; Eq. (41) can be used to refer the moment to a point that is not the mid-chord

Λ	A_n	B_n	C_n	D_n	E_n
$F(t,a)$	$Q_{\mathrm{T}}^{(0)}\{f_n;a\}$	$Q_{\mathrm{T}}^{(0)}\{\dot f_n;a\}+Q_{T}^{(0)}\{f_n;a\}$	$Q_{\mathrm{T}}^{(0)}\{\dot f_n;a\}$	$Q_{\widehat{\mathrm{T}}}^{(0)}\{f_n;a\}$	$Q_{\widehat{\mathrm{T}}}^{(0)}\{\dot f_n;a\}$
$M(t,a,0)$	$Q_{\mathrm{T}}^{(0)}\{f_n;a\}$	$Q_{\mathrm{T}}^{(1)}\{\dot f_n;a\}+Q_{T}^{(1)}\{f_n;a\}$	$Q_{\mathrm{T}}^{(1)}\{\dot f_n;a\}$	$Q_{\widehat{\mathrm{T}}}^{(1)}\{f_n;a\}$	$Q_{\widehat{\mathrm{T}}}^{(1)}\{\dot f_n;a\}$

Table 3
Coefficients for lift, $F(\bullet,-1)$, mid-chord pitching moment, $M(\bullet,-1,0)$, quarter-chord pitching moment, $M(\bullet,-1,-1/2)$, hinge force, $F(\bullet,1-2c_e)$, and hinge moment, $M(\bullet,1-2c_e,1-2c_e)$. All coefficients that are independent of the surface and tab chords are exact; the rest are leading order approximations

Parameter	DOF	n	A_n	B_n	C_n	D_n	E_n
Lift	z_{LE}	1	π	2π	0	-2π	0
	α	2	π	4π	2π	-3π	-2π
	δ_e	3	$\frac{64}{15}c_e^{5/2}$	$16c_e^{3/2}$	$8c_e^{1/2}$	$-\frac{32}{3}c_e^{3/2}$	$-8c_e^{1/2}$
	δ_t	4	$\frac{64}{15}c_e^{5/2}c_t^{5/2}$	$16c_e^{3/2}c_t^{3/2}$	$8c_e^{1/2}c_t^{1/2}$	$-\frac{32}{3}c_e^{3/2}c_t^{3/2}$	$-8c_e^{1/2}c_t^{1/2}$
Mid-chord pitching moment	z_{LE}	1	0	$\pi/2$	0	$-\pi/2$	0
	α	2	$-\pi/16$	$\pi/2$	$\pi/2$	$-3\pi/4$	$-\pi/2$
	δ_e	3	$-\frac{16}{15}c_e^{5/2}+\frac{8}{7}c_e^{7/2}$	$-\frac{4}{3}c_e^{3/2}+\frac{62}{15}c_e^{5/2}$	$\frac{8}{3}c_e^{3/2}$	$-\frac{8}{3}c_e^{3/2}$	$-2c_e^{1/2}$
	δ_t	4	$-\frac{16}{15}c_e^{5/2}c_t^{5/2}$	$-\frac{4}{3}c_e^{3/2}c_t^{3/2}$	$\frac{8}{3}c_e^{3/2}c_t^{3/2}$	$-\frac{8}{3}c_e^{3/2}c_t^{3/2}$	$-2c_e^{1/2}c_t^{1/2}$
Quarter-chord pitching moment	z_{LE}	1	$-\pi/4$	0	0	0	0
	α	2	$-5\pi/16$	$-\pi/2$	0	0	0
	δ_e	3	$-\frac{32}{15}c_e^{5/2}+\frac{8}{7}c_e^{7/2}$	$-\frac{16}{3}c_e^{3/2}+\frac{62}{15}c_e^{5/2}$	$-2c_e^{1/2}+\frac{8}{3}c_e^{3/2}$	0	0
	δ_t	4	$-\frac{32}{15}c_e^{5/2}c_t^{5/2}$	$-\frac{16}{3}c_e^{3/2}c_t^{3/2}$	$-2c_e^{1/2}c_t^{1/2}$	0	0
Hinge force	z_{LE}	1	$\frac{16}{3}c_e^{3/2}$	$\frac{8}{3}c_e^{3/2}$	0	$-\frac{8}{3}c_e^{3/2}$	0
	α	2	$8c_e^{3/2}$	$\frac{40}{3}c_e^{3/2}$	$\frac{8}{3}c_e^{3/2}$	$-4c_e^{3/2}$	$-\frac{8}{3}c_e^{3/2}$
	δ_e	3	$\frac{128}{9\pi}c_e^{3}$	$\frac{32}{\pi}c_e^{2}$	$\frac{8}{\pi}c_e$	$-\frac{128}{9\pi}c_e^{3}$	$-\frac{32}{3\pi}c_e^{2}$
	δ_t	4	$\frac{256}{15\pi}c_e^{3}c_t^{5/2}$	$\frac{128}{3\pi}c_e^{2}c_t^{3/2}$	$\frac{16}{\pi}c_ec_t^{1/2}$	$-\frac{128}{9\pi}c_e^{3}c_t^{3/2}$	$-\frac{32}{3\pi}c_e^{2}c_t^{1/2}$
Hinge moment	z_{LE}	1	$-\frac{32}{15}c_e^{5/2}$	$-\frac{16}{15}c_e^{5/2}$	0	$\frac{16}{15}c_e^{5/2}$	0
	α	2	$-\frac{16}{5}c_e^{5/2}$	$-\frac{16}{3}c_e^{5/2}$	$-\frac{16}{15}c_e^{5/2}$	$\frac{8}{5}c_e^{5/2}$	$\frac{16}{15}c_e^{5/2}$
	δ_e	3	$-\frac{64}{9\pi}c_e^{4}$	$-\frac{128}{9\pi}c_e^{3}$	$-\frac{8}{3\pi}c_e^{2}$	$\frac{256}{45\pi}c_e^{4}$	$\frac{64}{15\pi}c_e^{3}$
	δ_t	4	$-\frac{512}{45\pi}c_e^{4}c_t^{5/2}$	$-\frac{256}{9\pi}c_e^{3}c_t^{3/2}$	$-\frac{32}{3\pi}c_e^{2}c_t^{1/2}$	$\frac{256}{45\pi}c_e^{4}c_t^{3/2}$	$\frac{64}{15\pi}c_e^{3}c_t^{1/2}$

loads, that are associated with surface and tab deflections, are attenuated by c_e (for those $k=1$ by Table 4); hence it is plausible that they may turn out to be negligible for sufficiently small surface chord. This point will be discussed, in detail, in the next section.

Under the assumption that no wing motion occurred prior to time $t=0$, Laplace transform of Eq. (85) yields

$$\begin{aligned}L\{\Lambda-\Lambda_0;s\}&=(-1)^l c_e^{n/2}(a_1s^2+b_1s+c_1s-(d_1s+e_1)\hat P_0(s))L\{z_{\mathrm{LE}};s\}+(-1)^l c_e^{n/2}(a_2s^2+b_2s+c_2-(d_2s+e_2)\hat P_0(s))\\&\quad\times L\{\alpha;s\}+(-1)^l c_e^{(n+m)/2}(a_3c_e^2s^2+b_3c_es+c_3-c_e^k(d_3c_es+e_3)\hat P_0(s))L\{\delta_e;s\}\\&\quad+(-1)^l c_e^{(n+m)/2}c_t^{1/2}(a_4c_e^2c_t^2s^2+b_4c_ec_ts+c_4\delta_t-c_e^k(d_4c_ec_ts+e_4)\hat P_0(s))L\{\delta_t;s\}.\end{aligned}\tag{86}$$

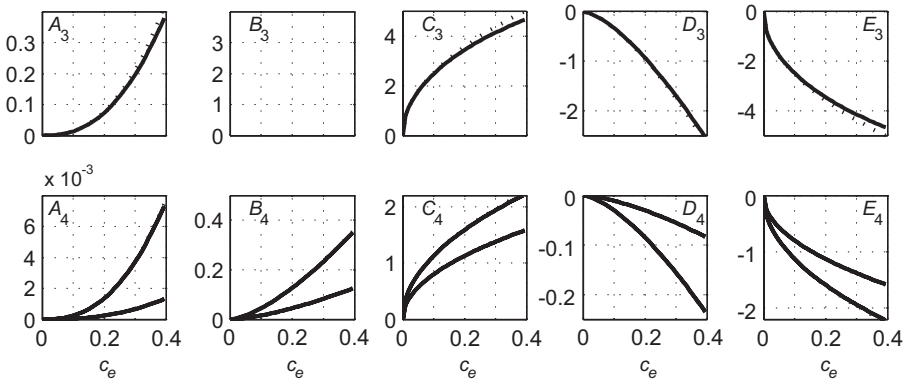

Fig. 4. Lift force $F(\bullet,-1)$ coefficients as functions of c_e; in the second line, c_t equals 0.1 (smaller absolute values) and 0.2. Dotted lines mark approximations of Table 3. $A_1,\ldots,E_2$ are not shown since they are independent of c_e.

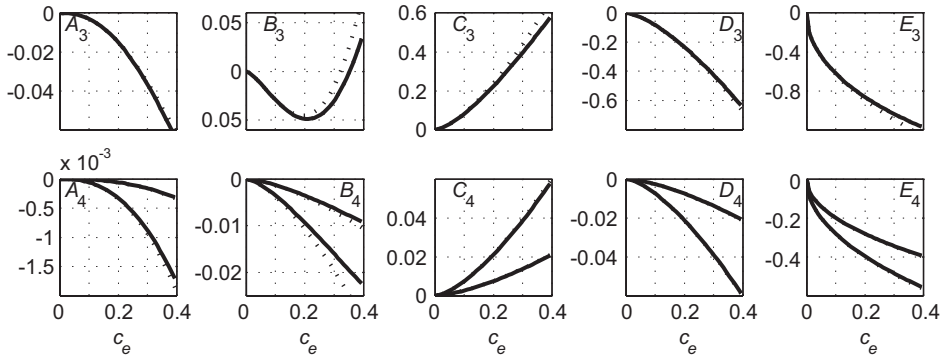

Fig. 5. Mid-chord pitching moment $M(\bullet,-1,0)$ coefficients as functions of c_e; in the second line, c_t equals 0.1 (smaller absolute values) and 0.2. Dotted lines mark approximations of Table 3. $A_1,\ldots,E_2$ are not shown since they are independent of c_e.

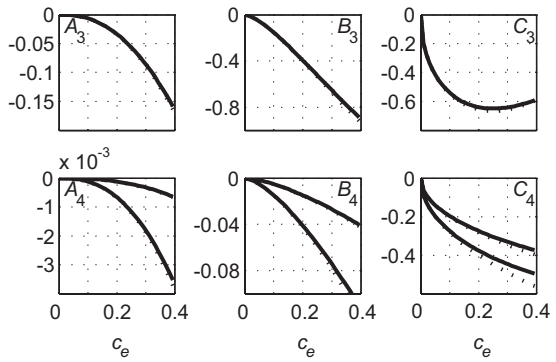

Fig. 6. Quarter-chord pitching moment $M(\bullet,-1,-1/2)$ coefficients as functions of c_e; in the second line, c_t equals 0.1 (smaller absolute values) and 0.2. Dotted lines mark approximations of Table 3. $A_1,\ldots,E_2$ are not shown since they are independent of c_e; D_3, D_4, E_3 and E_4 are identically zero.

The values of $\hat{P}_0$ are mapped in Fig. 9 over the first quarter of the complex plane; its real and imaginary parts are, respectively, symmetric and anti-symmetric with respect to the real axis. The absolute value of $\hat{P}_0$ is bounded by 1/2 on the right-half plane; its asymptotic behavior is given by Eqs. (35) and (36). Hence history-dependent effects bear no consequence on the aerodynamic loads at high and low frequencies alike; for rapid motions (large s), added-mass effects are dominant; for slow motions (small s) aerodynamic stiffness is dominant. In between these limits, history-dependent effects act so as to reduce both damping and stiffness.

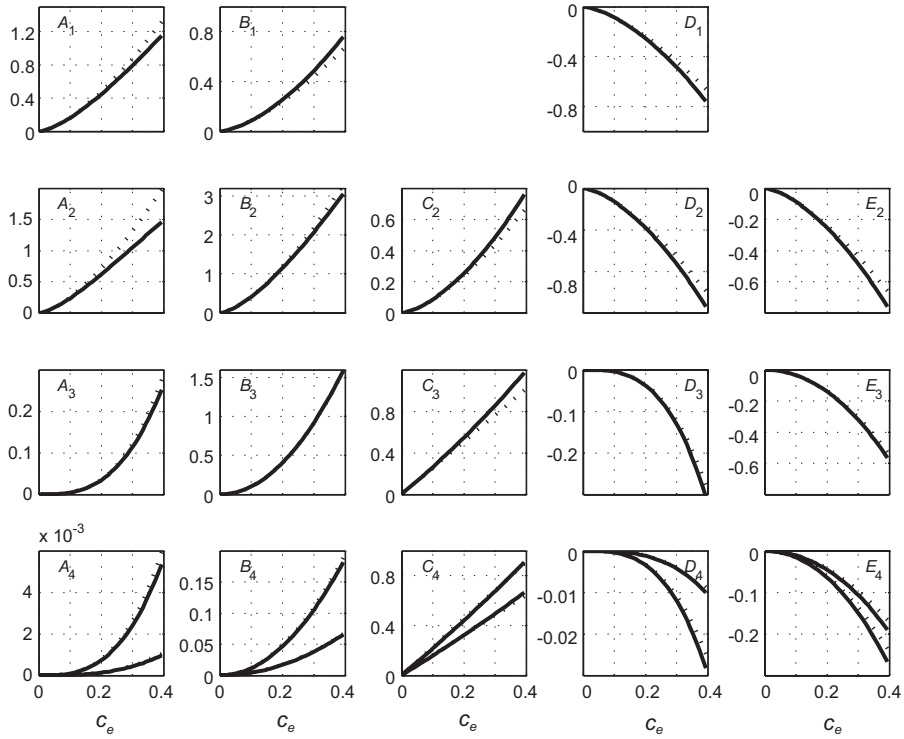

Fig. 7. Hinge force $F(\bullet, 1-2c_e)$ coefficients as functions of surface chord fraction c_e; dotted lines mark the approximations of Table 3; in the bottom line, tab chord fraction c_t equals 0.1 (smaller absolute values) and 0.2. C_1 and E_1 are identically zero.

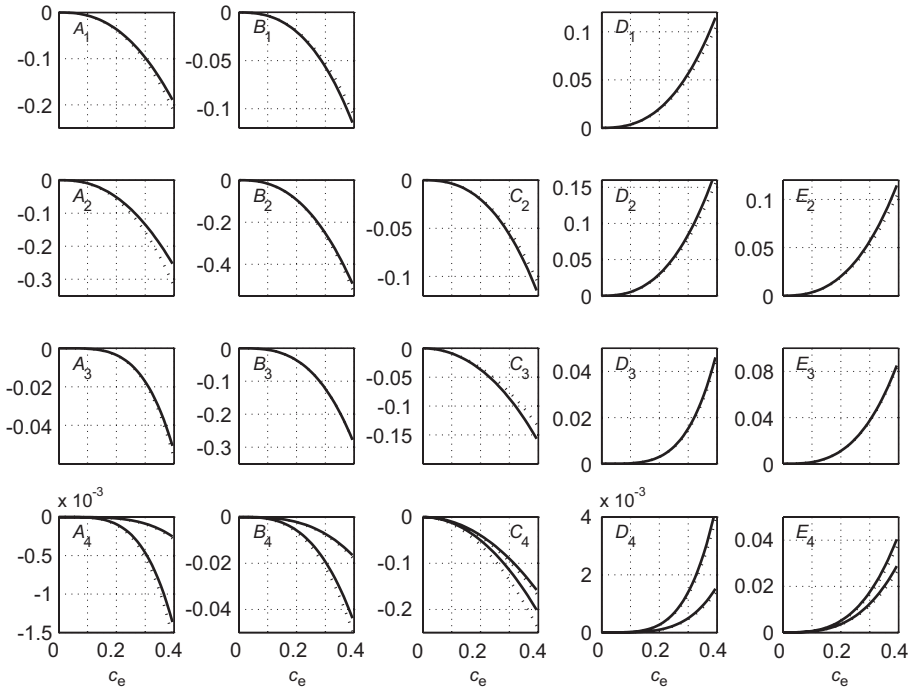

Fig. 8. Hinge moment $M(\bullet, 1-2c_e, 1-2c_e)$ coefficients as functions of surface chord fraction c_e; dotted lines mark the approximations of Table 3; in the bottom line, tab chord fraction c_t equals 0.1 (smaller absolute values) and 0.2. C_1 and E_1 are identically zero.

Table 4
Powers in Eq. (85)

Parameter	k	l	m	n
Lift	0	0	1	0
Quarter-chord pitching moment	n/a	1	1	0
Hinge force	1	0	−1	3
Hinge moment	1	1	−1	5

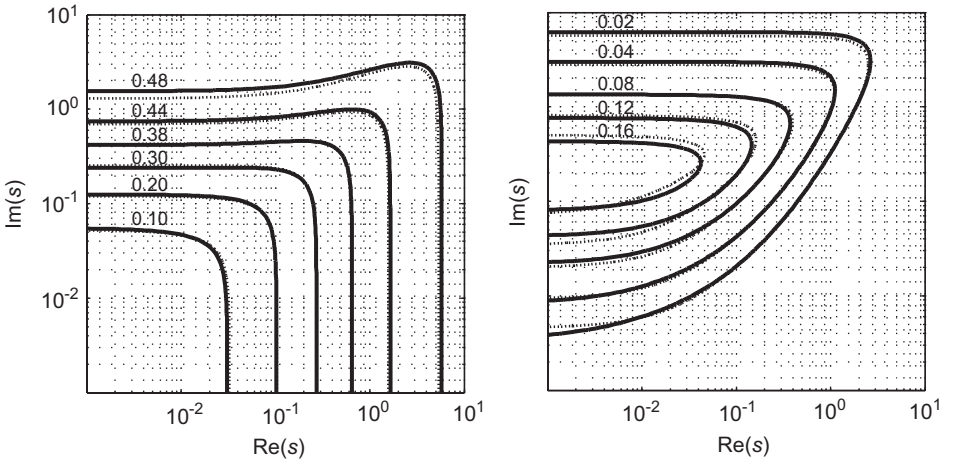

Fig. 9. Function $\hat{P}_0$ over the upper-right quarter of the complex plane. Real part of the function is shown on the left; imaginary part is shown on the right. Rational approximation (87) of $\hat{P}_0$ is marked by broken lines.

In relation to $\hat{P}_0$, two comments are in order. The first one concerns its equivalence with the generalized Theodorsen's function $s \to C(-\mathrm{i}s)$, used, for example, in Edwards et al. (1979). In fact, $C(-\mathrm{i}s) = 1 - \hat{P}_0(s)$, by Eqs. (65), (34) and (63). We believe that the vanishing of $\hat{P}_0$ at small frequencies makes it more convenient to work with than with $s \to C(-\mathrm{i}s)$; in particular, it facilitates its approximation. And that leads to the second comment.

A rational (Pade) approximation of a standard response function will be customary constructed by fitting its Laplace transform with a ratio of two polynomials over a segment of the imaginary axis. We suggest fitting it over a segment of the Bromwich contour instead. While it will make no difference for converging responses — where the Bromwich contour can be chosen along the imaginary axis — it can improve approximation accuracy for diverging responses.

A simple second-order approximation

$$\hat{P}_{0,\mathrm{r}}(s) = \frac{0.2097s}{s + 0.0584} + \frac{0.2903s}{s + 0.3478}, \tag{87}$$

fits nicely the real and imaginary constituents of $\hat{P}_0$ over the entire right half plane—see Fig. 9. As compared with second-order approximation based on the standard Jones approximation (fitting $k \to C(k)$)—see Bisplinghoff et al. (1996, p. 285). Eq. (87) offers a similar fit over the entire imaginary axis and a better fit to the right of it.

9. Control with tabs—a naïve approach

All this can now be elucidated by solving a simple practical problem—the one that actually triggered this study. A control surface is held at zero deflection by an actuator, that initially counterbalances the aerodynamic hinge moment, $M(0, h_\mathrm{e}, h_\mathrm{e})$, acting on the surface. At $t = 0$ the actuator fails (breaks), leaving the surface with no damping and no friction. After the new steady state has been set, the control over the surface is regained by means of the trim tab.

In this scenario, two points are of interest. One concerns the transient response of the surface immediately after the actuator failure; the other concerns the lag between tab command and the resulting response of the control surface.

Let j be the (dimensionless) moment of inertia per unit span of the surface. It is plausible that j should depend on the surface chord squared and the mass of the surface per unit of its span. Since the latter depends itself on the effective cross section area, we may set, without loss of generality,

$$j = \bar{j} c_e^4, \tag{88}$$

where $\bar{j}$ is a certain (dimensionless) parameter. If the mass of the surface is concentrated in its upper and lower skins, each of effective (dimensionless) thickness t_s, and (real, not dimensionless) density ρ_s, one should find no difficulty to verify that

$$\bar{j} = \frac{8}{3}\frac{\rho_s}{\rho}\frac{t_s}{c_e}. \tag{89}$$

Given aluminum-to-air densities ratio of about 2200 at sea level, and effective skin thickness to surface chord ratio of 0.004 (1 mm skin with 500 mm surface chord; recall that t_s is referred to the wing semi-chord, whereas c_e is referred to the wing chord), $\bar{j}$ turns out to be about 27; it increases four-fold at 40 000 ft (~12 200 m) altitude.

Neglecting airframe dynamics as well as friction and damping of the failed actuator, the equation of motion governing the surface deflection after the failure is simply

$$\begin{aligned}\bar{j} c_e^2 \ddot{\delta}_e(t) = {} & c_e^2 c_3 \delta_\infty \mathscr{H}(t) - c_e^2 (a_3 c_e^2 \ddot{\delta}_e(t) + b_3 c_e \dot{\delta}_e(t) + c_3 \delta_e(t) - c_e (d_3 c_e W\{\dot{\delta}_e; t\} + e_3 W\{\delta_e; t\})) \\ & - c_e^2 c_t^{1/2} (a_4 c_e^2 c_t^2 \ddot{\delta}_t(t) + b_4 c_e c_t \dot{\delta}_t(t) + c_4 \delta_t(t) - c_e (d_4 c_e c_t W\{\dot{\delta}_t; t\} + e_4 W\{\delta_t; t\})),\end{aligned} \tag{90}$$

where the coefficients $a_3, \ldots, e_4$ are those pertaining to the hinge moment $M(t, h_e, h_e)$, whereas

$$\delta_\infty = -M(0, h_e, h_e)/(c_3 c_e^2) \tag{91}$$

is the equilibrium deflection of the control surface after actuator failure.

Given that for all $t \leqslant 0$, both control and tab surfaces had zero deflection, solution of Eq. (90) is straightforward. Starting with the Laplace transform, one has that

$$L\{\delta_e; s\} = \frac{1}{s}\hat{H}_0^e(c_e s, c_e)\delta_\infty + c_t^{1/2}\hat{H}_0^t(c_e s, c_e) L\{-\delta_t; s\}, \tag{92}$$

where

$$\hat{H}_0^e(s, c_e) = \frac{c_3}{(a_3 + \bar{j})s^2 + b_3 s + c_3 - (d_3 s + e_3) c_e \hat{P}_0(s/c_e)}, \tag{93}$$

$$\hat{H}_0^t(s, c_e) = \frac{a_4 c_t^2 s^2 + b_4 c_t s + c_4 - (d_4 c_t s + e_4) c_e \hat{P}_0(s/c_e)}{(a_3 + \bar{j})s^2 + b_3 s + c_3 - (d_3 s + e_3) c_e \hat{P}_0(s/c_e)}, \tag{94}$$

are the respective transfer functions. Hence, given standard (reduced) responses of the control surface,

$$H_n^{e,t}(t, c_e) = \int_{\gamma - i\infty}^{\gamma + i\infty} \hat{H}_0^{e,t}(s, c_e) \frac{e^{st}}{s^n}\, ds, \tag{95}$$

to an impulse ($n = 0$), step ($n = 1$), etc., inverse transform of Eq. (92) yields the solution of (90) as

$$\delta_e(t) = \delta_\infty H_1^e((t - \tau)/c_e, c_e) - \frac{c_t^{1/2}}{c_e}\int_0^t H_0^t((t - \tau)/c_e, c_e)\, \delta_t(\tau)\, d\tau. \tag{96}$$

Now, all coefficients appearing in Eqs. (93) and (94) are positive, and, in particular, a_3, b_3 and c_3—cf. the paragraph following Eq. (85). With positive coefficients, the roots of $(a_3 + \bar{j})s^2 + b_3 s + c_3$ lay on the left half-plane. Noting Eq. (36), this information is sufficient to expand $\hat{H}_0^e$ and $\hat{H}_0^t$ about $c_e = 0$ on the right half-plane to obtain

$$\hat{H}_0^e(s, c_e) = \hat{H}_0^e(s, 0)\left(1 + \frac{d_3 s + e_3}{(a_3 + \bar{j})s^2 + b_3 s + c_3}\frac{c_e}{2} + \cdots\right), \tag{97}$$

$$\hat{H}_0^t(s, c_e) = \hat{H}_0^t(s, 0)\left(1 + \left(\frac{d_3 s + e_3}{(a_3 + \bar{j})s^2 + b_3 s + c_3} - \frac{d_4 c_t s + e_4}{a_4 c_t^2 s^2 + b_4 c_t s + c_4}\right)\frac{c_e}{2} + \cdots\right). \tag{98}$$

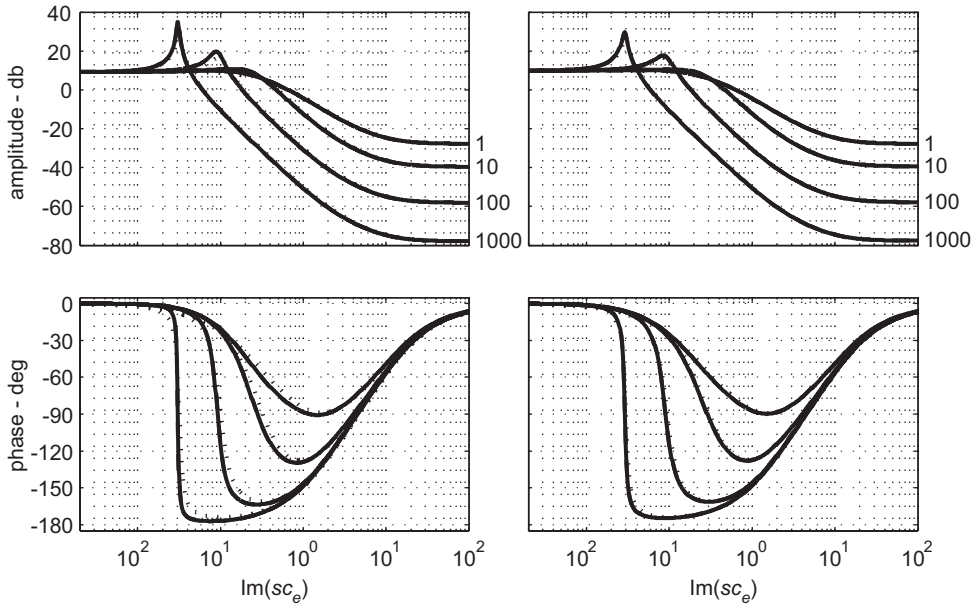

Fig. 10. Bode plots of $\hat{H}_0^{\mathrm{t}}(\bullet, c_{\mathrm{e}})$ with $c_{\mathrm{e}} = 0.4$ (left) and $c_{\mathrm{e}} = 0.15$ (right), $c_{\mathrm{t}} = 0.2$ for four different $\bar{j}$'s; their values appear to the right of the respective lines. Dotted lines mark the approximation where all history-dependent terms have been neglected. Dashed lines, practically indistinguishable from the solid lines, mark second-order rational approximation (87) of $\hat{P}_0$.

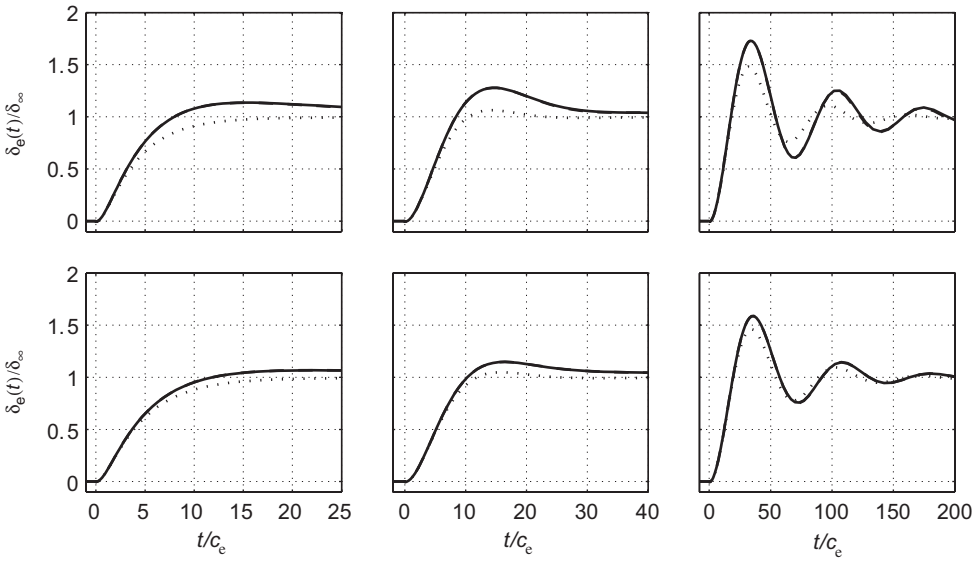

Fig. 11. Time response of 40% (top) and 15% (bottom) chord control surfaces to a step in the hinge moment. The three columns correspond to three different values of $\bar{j}$, starting with 1 on the left, 10 in the middle and 100 on the right. Dotted line mark time response computed neglecting all history-dependent effects. Rational approximation (87) is marked by dashed lines, they are indistinguishable from the exact ones.

History-dependent effects in Eqs. (93) and (94) are embodied in the terms involving $\hat{P}_0$; these terms are associated with the coefficients d_3, d_4, e_3 and e_4. Since these coefficients are absent from Eqs. (97) and (98) in the leading order with respect to c_{e}, one must conclude that for sufficiently small surface chord to total chord ratio, history-dependent effects can be neglected altogether. The particular value of c_{e}, rendering this approximation valid, depends on the roots of the polynomial $(a_3 + \bar{j})s^2 + b_3 s + c_3$; the closer these are to the imaginary axis, the smaller this value of c_{e} will be.

Typical history-related effects are shown in Figs. 10 and 11 for 15% and 40% chord surfaces, equipped with 20% surface-chord tab. Since aileron chord rarely exceeds 20% of the respective wing-chord, the problem of controlling an aileron with a tab can probably be adequately analyzed neglecting all history-dependent effects. At the same time, elevator chord to total chord ratio is typically large, and hence history-less analysis should be done with caution. Whenever in doubt, a rational approximation (87) for $\hat{P}_0$ seems adequate, yielding Bode diagrams of $\hat{H}_0^{\mathrm{t}}(\bullet, c_{\mathrm{e}})$ (Fig. 10), and time responses $H_1^{\mathrm{e}}(\bullet)$ (Fig. 11) practically indistinguishable from the exact ones.

Ailerons on supercritical wings are known to have an upward-sucking hinge moment, causing the free floating angle δ_∞ at cruise conditions to be almost at the hard stop. The responses shown in Fig. 11 imply that if the actuator fails at cruising altitude, where $\bar{j}$ is large, this free floating angle will be reached with a significant angular rate. Loosely speaking, the aileron will hit its hard stop with a great 'bang'. The energy of this impact (per unit span and normalized by $2\rho U^2 b^2$) can be bounded by $M(0, h_{\mathrm{e}}, h_{\mathrm{e}})^2/(2c_3 c_{\mathrm{e}}^2)$, the energy stored in the actuator under the assumption of linear aerodynamics. Artificial damping of the aileron is, therefore, a necessity. But if damping is added, its slower response will render all pertinent history-dependent effects totally insignificant.

10. Conclusions

This exposition can be conceptually divided into three parts, the first two addressing aerodynamics and the last one addressing the actual response of the control surface. In its first part, integral aerodynamic loads acting on an arbitrary moving, not necessarily rigid, wing, have been obtained. The solution was based on Laplace transform and recovers the results of Sears (1940) as its sub-case. The most conspicuous results of this part are, perhaps, the standard circulation response functions, G_n—cf. (21)—and pressure response functions, P_n—cf. Eq. (33)—to unit impulse ($n = 0$), unit step ($n = 1$), etc. in normal-to-the-wing velocity. G_n convolves with the nth derivative of the latter with respect to time to yield history-dependent constituent of the circulation about the wing (20); P_n convolves with the same derivative to yield the history-dependent constituent of the aerodynamic forces (30), (55), (56), (85). The function $t \to \mathscr{H}(t) - \mathrm{P}_1(t)$ has been identified with the Wagner function; the function G_1 has been identified with the Küssner function.

It is believed that the work with the functions P_n in general, and with P_1 in particular, is more convenient than the work with the Wagner function. The former vanishes at long times, whereas the latter goes to unity. This property of P_1 both facilitates its approximation, and makes explicit the vanishing of the far-wake (or far-history) effects on the aerodynamic loads. Similarly, it is believed that the work with the functions $\hat{P}_n$ in general (the respective transforms of P_n), and with $\hat{P}_0$ in particular, is more convenient than the work with the function $s \to C(-\mathrm{i}s) = 1 - \hat{P}_0(s)$ based on analytical continuation of the Theodorsen's function (65) over the right-half plane. The former vanishes for the quasisteady limit whereas the latter goes to unity.

Rational approximations of a function are customarily constructed by curve-fitting it along the imaginary axis—e.g. Edwards et al. (1979). Indeed, in the vast majority of the cases, converging responses may be computed using no offset of the Bromwich contour from the imaginary axis, and in those cases the common practice is, of course, a valid one. However, computation of diverging responses will require an offset of the Bromwich contour to the right of the imaginary axis; in those cases the common practice becomes inaccurate. A better solution can be obtained by curve-fitting $\hat{P}_n$ along the Bromwich contour—the actual contour on which the inverse transform is constructed.

In the second part of the paper, integral aerodynamic loads acting on any part of a three-segment wing have been obtained in a closed analytical form—cf. Eqs. (82), (83) and (84) in conjunction with Eqs. (C.1)–(C.12). For the case of harmonic oscillations, these closed-form results recover those found in most current references, hopefully in somewhat more ordered form. Still, the exact analytical expressions have been found too lengthy to be used in analysis, and hence simplified, easy-to-use approximations have been suggested instead—cf. Eq. (84) in conjunction with Table 3. It seems that these approximations are accurate enough for all practical purposes.

In the third part of the paper, the results of the second part were used to obtain the time response of the control surface to actuator failure and to subsequent control input of the tab surface; cf. (96) and Figs. 10 and 11. The most conspicuous conclusion here is that history-dependent effects can be neglected as long as the chord of the control surfaces is sufficiently small compared to the total chord. Practically, it means that the ailerons can be analyzed history-free, whereas large elevator will typically require all effects to be included.

Acknowledgment

This work was supported, in part, by the European Commission Research Directorates, Framework V, GROWTH Project No. GRD1-2000-25261. The help of Dr Ehud Yariv from Department of Mechanical Engineering during the initial stages of this research is appreciated.

Appendix A. Some typical integrals

Throughout this Appendix, n and m are any nonnegative integers, a, b, h, x and ζ are any real numbers in the interval $(-1, 1)$, ξ is any real number in the interval $(1, \infty)$; Λ_1 and Λ_2 are functions that have been defined in Eqs. (25) and (26), respectively; M_n and N_n are integral operators that have been defined in Eqs. (47) and (48), respectively; $\mathscr{H}$ is the Heaviside step function; and angular brackets are used to imply truncation of the negative values, e.g. $\langle x\rangle = x\mathscr{H}(x)$; and, finally, s_b^n and S_b^n are functions on $[-1,1]$, such that $s_b^n(x) = (x-b)^n$ and $S_b^n(x) = \langle x-b\rangle^n$. Pertinent integrals are:

$$\fint_{-1}^{1}\sqrt{\frac{1-x}{1+x}}\frac{\mathrm{d}x}{x-\zeta} = -\pi, \tag{A.1}$$

$$\fint_{-1}^{1}\sqrt{\frac{1-x}{1+x}}\frac{\mathrm{d}x}{x-\xi} = -\pi + \pi\sqrt{\frac{\xi-1}{\xi+1}}, \tag{A.2}$$

$$\fint_{-1}^{a}\sqrt{\frac{1-x}{1+x}}\frac{\mathrm{d}x}{x-\zeta} = \cos^{-1}a - \pi - \sqrt{\frac{1-\zeta}{1+\zeta}}\Lambda_1(a,\zeta), \tag{A.3}$$

$$\fint_{-1}^{a}\sqrt{\frac{1-x}{1+x}}\frac{\mathrm{d}x}{x-\xi} = \cos^{-1}a - \pi - \sqrt{\frac{\xi-1}{\xi+1}}\left(2\Lambda_2(a,\xi) + \cos^{-1}a - \pi\right), \tag{A.4}$$

$$\fint_{a}^{1}\sqrt{\frac{1-x}{1+x}}\frac{\mathrm{d}x}{x-\zeta} = -\cos^{-1}a + \sqrt{\frac{1-\zeta}{1+\zeta}}\Lambda_1(a,\zeta), \tag{A.5}$$

$$\fint_{a}^{1}\sqrt{\frac{1-x}{1+x}}\frac{x-h}{x-\zeta}\mathrm{d}x = \cos^{-1}a - \sqrt{1-a^2} - (\zeta-h)\left(\cos^{-1}a - \sqrt{\frac{1-\zeta}{1+\zeta}}\Lambda_1(a,\zeta)\right), \tag{A.6}$$

$$\fint_{a}^{1}\Lambda_1(x,\zeta)\mathrm{d}x = (\zeta-a)\Lambda_1(a,\zeta) + \sqrt{1-\zeta^2}\cos^{-1}a, \tag{A.7}$$

$$\fint_{a}^{1}\Lambda_1(x,\zeta)(x-h)\mathrm{d}x = \frac{1}{2}(\zeta-a)(\zeta+a-2h)\Lambda_1(a,\zeta) + \frac{1}{2}\sqrt{1-\zeta^2}\left((\zeta-2h)\cos^{-1}a + \sqrt{1-a^2}\right), \tag{A.8}$$

$$\int_{a}^{1}\sqrt{\frac{1-x}{1+x}}\mathrm{d}x = \cos^{-1}a - \sqrt{1-a^2}, \tag{A.9}$$

$$\int_{a}^{1}\sqrt{\frac{1-x}{1+x}}(x-h)\mathrm{d}x = \frac{1}{2}\left(-(2h+1)\cos^{-1}a + (2+2h-a)\sqrt{1-a^2}\right), \tag{A.10}$$

$$M_0\{S_a^0\} = \int_{a}^{1}\sqrt{\frac{1+\zeta}{1-\zeta}}\mathrm{d}\zeta = \cos^{-1}a + \sqrt{1-a^2}, \tag{A.11}$$

$$M_1\{S_a^0\} = \int_{a}^{1}\sqrt{1-\zeta^2}\mathrm{d}\zeta = \frac{1}{2}\left(\cos^{-1}a - a\sqrt{1-a^2}\right), \tag{A.12}$$

$$M_2\{S_a^0\} = \int_{a}^{1}\sqrt{1-\zeta^2}(1-\zeta)\mathrm{d}\zeta = \frac{1}{6}\left(3\cos^{-1}a - \left(2+3a-2a^2\right)\sqrt{1-a^2}\right), \tag{A.13}$$

$$M_3\{S_a^0\} = \int_{a}^{1}\sqrt{1-\zeta^2}(1-\zeta)^2\mathrm{d}\zeta = \frac{1}{24}\left(15\cos^{-1}a - \left(16+9a-16a^2+6a^3\right)\sqrt{1-a^2}\right), \tag{A.14}$$

$$M_n\{S_a^1\} = \int_{a}^{1}\sqrt{\frac{1+\zeta}{1-\zeta}}(\zeta-a)(1-\zeta)^n\mathrm{d}\zeta = (1-a)M_n\{S_a^0\} - M_{n+1}\{S_a^0\}, \tag{A.15}$$

$$M_n\{1\} = M_n\{S^0_{-1}\}, \tag{A.16}$$

$$M_n\{s^1_h\} = M_n\{S^1_{-1}\} - (1+h)M_n\{1\}, \tag{A.17}$$

$$N_n\{S^0_b; a\} = \fint_b^1 (\zeta - a)^n \Lambda_1(a,\zeta)\,\mathrm{d}\zeta = \frac{1}{n+1}\left(-(b-a)^{n+1}\Lambda_1(a,b) + \sqrt{1-a^2}\int_b^1 \frac{(\zeta-a)^n}{\sqrt{1-\zeta^2}}\mathrm{d}\zeta\right), \tag{A.18}$$

$$N_0\{S^0_b; a\} = \cos^{-1} b\sqrt{1-a^2} + (a-b)\Lambda_1(a,b), \tag{A.19}$$

$$N_1\{S^0_b; a\} = \frac{\sqrt{1-a^2}}{2}\left(\sqrt{1-b^2} - a\cos^{-1} b\right) - \frac{(a-b)^2}{2}\Lambda_1(a,b), \tag{A.20}$$

$$N_2\{S^0_b; a\} = \frac{\sqrt{1-a^2}}{6}\left(\left(2a^2+1\right)\cos^{-1} b - (4a-b)\sqrt{1-b^2}\right) + \frac{(a-b)^3}{3}\Lambda_1(a,b), \tag{A.21}$$

$$N_3\{S^0_b; a\} = \frac{\sqrt{1-a^2}}{24}\left(\left(2b^2+4-9ab+18a^2\right)\sqrt{1-b^2} - a\left(6a^2+9\right)\cos^{-1} a\right) - \frac{(a-b)^4}{4}\Lambda_1(a,b), \tag{A.22}$$

$$N_n\{S^1_b; a\} = \fint_b^1 (\zeta-a)^n(\zeta-b)\Lambda_1(a,\zeta)\mathrm{d}\zeta = N_{n+1}\{S^0_b; a\} + (a-b)N_n\{S^0_b; a\}, \tag{A.23}$$

$$N_n\{1; a\} = \fint_{-1}^1 (\zeta-a)^n\Lambda_1(a,\zeta)\mathrm{d}\zeta = N_n\{S^0_{-1}; a\}, \tag{A.24}$$

$$N_n\{s^1_h; a\} = \fint_{-1}^1 (\zeta-a)^n(\zeta-h)\Lambda_1(a,\zeta)\mathrm{d}\zeta = N_{n+1}\{1; a\} + (a-h)N_n\{1; a\}. \tag{A.25}$$

Appendix B. The gust problem

This appendix addresses the problem of aerodynamic loads exerted on a wing in steady motion through stationary (time independent as viewed from a stationary reference frame) nonuniform vertical gust of velocity v—see Bisplinghoff et al. (1996, p. 286). The only difference between this problem (to be loosely referred to as the 'gust problem') and that of a wing in unsteady motion through uniform air, is in the impermeability condition, with

$$\frac{1}{2\pi}\fint_{-1}^{\infty}\frac{\partial\mu(t,x')}{\partial x'}\frac{\mathrm{d}x'}{x-x'} = v(t-x-1) \tag{B.1}$$

replacing Eq. (5) as the condition to be satisfied for each x in (-1, 1). Here, the argument of v was chosen so that if

$$v(\zeta) = 0 \tag{B.2}$$

for each $\zeta \le 0$, the leading edge of the wing will hit the edge of the gust at time $t = 0$. Without loss of generality, this assumption will be tacitly assumed below.

The similarity between the gust problem and that solved in Sections 3–5 allows obtaining all aerodynamic loads by merely repeating the steps leading to Eqs. (20), (30), (42) and (43) with $v(t-x-1)$ instead of $X(x)T(t)$. The details follow.

First, separate the wing contribution in Eq. (B.1) from that of the wake, and use Eq. (3) to obtain

$$\frac{1}{2\pi}\fint_{-1}^{1}\frac{\partial\mu(t,x')}{\partial x'}\frac{\mathrm{d}x'}{x-x'} = v(t-x-1) + \frac{1}{2\pi}\int_1^{1+t}\frac{\mathrm{d}\mu_{\mathrm{TE}}(t-x'+1)}{\mathrm{d}t}\frac{\mathrm{d}x'}{x-x'} \tag{B.3}$$

for each x in $(-1, 1)$; it is an equivalent of Eq. (9). In analogy with the latter, the solution of Eq. (B.3), having square-root singularity at the leading edge and finite at the trailing edge, is

$$\frac{\partial\mu(t,x)}{\partial x} = -\frac{2}{\pi}\sqrt{\frac{1-x}{1+x}}\fint_{-1}^{1}\sqrt{\frac{1+\zeta}{1-\zeta}}\frac{v(t-\zeta-1)\mathrm{d}\zeta}{x-\zeta} + \frac{1}{\pi}\sqrt{\frac{1-x}{1+x}}\int_1^{1+t}\sqrt{\frac{\zeta+1}{\zeta-1}}\frac{\mathrm{d}\mu_{\mathrm{TE}}(t-\zeta+1)}{\mathrm{d}t}\frac{\mathrm{d}\zeta}{x-\zeta}. \tag{B.4}$$

Next, integrate on both sides of Eq. (B.4) with respect to x between -1 and 1; using Eqs. (4) and (8) the result can be brought into the form,

$$\int_1^{1+t}\sqrt{\frac{\zeta+1}{\zeta-1}}\frac{\mathrm{d}\mu_{\mathrm{TE}}(t-\zeta+1)}{\mathrm{d}t}\mathrm{d}\zeta=2\int_{-1}^{1}\sqrt{\frac{1+x}{1-x}}\,v(t-x-1)\mathrm{d}x, \tag{B.5}$$

it is an equivalent of Eq. (12). Applying Laplace transform on both sides, we immediately arrive at same left-hand-side as in Eq. (16),

$$s\mathrm{e}^{s}(\mathrm{K}_0(s)+\mathrm{K}_1(s))L\{\mu_{\mathrm{TE}};s\}=2\int_0^{\infty}\mathrm{e}^{-st}\mathrm{d}t\int_{-1}^{1}\sqrt{\frac{1+x}{1-x}}\,v(t-x-1)\mathrm{d}x. \tag{B.6}$$

Changing the order of integration, and employing that $v(t-x-1)=0$ for any $t<x+1$ byEq. (B.2), the integral on the right will be identified with a combination of Bessel functions of zero and first order; i.e.

$$\begin{aligned}\int_0^{\infty}\mathrm{e}^{-st}\mathrm{d}t\int_{-1}^{1}\sqrt{\frac{1+x}{1-x}}v(t-x-1)\mathrm{d}x&=\int_{-1}^{1}\sqrt{\frac{1+x}{1-x}}\mathrm{d}x\int_{x+1}^{\infty}\mathrm{e}^{-st}v(t-x-1)\mathrm{d}t\\&=\int_0^2\frac{x\mathrm{e}^{-sx}dx}{\sqrt{x(2-x)}}\int_0^{\infty}\mathrm{e}^{-s\tau}v(\tau)\mathrm{d}\tau=L\{v;s\}\int_0^2\frac{x\mathrm{e}^{-sx}\mathrm{d}x}{\sqrt{x(2-x)}}\\&=-L\{v;s\}\frac{\mathrm{d}}{\mathrm{d}s}\int_0^2\frac{x\mathrm{e}^{-sx}\mathrm{d}x}{\sqrt{x(2-x)}}=\pi L\{v;s\}\mathrm{e}^{-s}(\mathrm{I}_0(s)-\mathrm{I}_1(s));\end{aligned} \tag{B.7}$$

cf. Gradshteyn and Ryzhik (1980, Arts. 3.364.1 and 8.486.9). Thus,

$$L\{\mu_{\mathrm{TE}};s\}=2\pi\hat{g}_n(s)s^nL\{v;s\}, \tag{B.8}$$

with

$$\hat{g}_n(s)=\frac{\mathrm{e}^{-2s}}{s^{n+1}}\frac{\mathrm{I}_0(s)-\mathrm{I}_1(s)}{\mathrm{K}_0(s)+\mathrm{K}_1(s)}=\hat{G}_n(s)\mathrm{e}^{-s}(\mathrm{I}_0(s)-\mathrm{I}_1(s)), \tag{B.9}$$

cf. Eqs. (17) and (18). Therefore, in analogy with Eqs. (20) and (21),

$$\mu_{\mathrm{TE}}(t)=2\pi\int_0^t g_n(t-\tau)\frac{\mathrm{d}^nv(\tau)}{\mathrm{d}\tau^n}d\tau, \tag{B.10}$$

where

$$g_n(t)=L^{-1}\{\hat{g}_n;t\}. \tag{B.11}$$

Similar with their upper-case counterparts, g_0, g_1, … represent standard circulation responses to a unit gust impulse, gust step, etc. With $\hat{g}_n(s)$ behaving as s^{-n} for small s, and as $(1/4\pi s^{2+n})$ for large s, doublet ($n=-1$), impulse ($n=0$) and step ($n=1$) responses remain finite at all times. Higher-order responses diverge when t goes to infinity, lower order diverge when t goes to zero. Functions g_0 and g_1 are shown in Fig. B1.

Computation of the pressure jump requires both coordinate and time derivatives of μ. The former is given by Eq. (B.4); the latter is obtained by following the same steps as those leading to Eq. (27); the result is

$$\frac{\partial\mu(t,x)}{\partial t}=\frac{2}{\pi}\fint_{-1}^{1}\Lambda_1(x,\zeta)\frac{\mathrm{d}v(t-\zeta-1)}{\mathrm{d}t}\mathrm{d}\zeta+\frac{1}{\pi}\int_1^{1+t}\sqrt{\frac{1-x^2}{\zeta^2-1}}\frac{\mathrm{d}\mu_{\mathrm{TE}}(t-\zeta+1)}{\mathrm{d}t}\frac{\mathrm{d}\zeta}{\zeta-x}. \tag{B.12}$$

Thus

$$p(t,x)=\frac{4}{\pi}\sqrt{\frac{1-x}{1+x}}\fint_{-1}^{1}\sqrt{\frac{1+\zeta}{1-\zeta}}\frac{v(t-\zeta-1)\mathrm{d}\zeta}{x-\zeta}-\frac{4}{\pi}\fint_{-1}^{1}\Lambda_1(x,\zeta)\frac{\mathrm{d}v(t-\zeta-1)}{\mathrm{d}t}\mathrm{d}\zeta+\frac{2}{\pi}\sqrt{\frac{1-x}{1+x}}\int_1^{1+t}\frac{\mathrm{d}\mu_{\mathrm{TE}}(t-\zeta+1)}{\mathrm{d}t}\frac{\mathrm{d}\zeta}{\sqrt{\zeta^2-1}}; \tag{B.13}$$

it is an equivalent of Eq. (28). It can be somewhat simplified by integrating by parts in the second term on the right; in view of Eqs. (A.6) and (B.2) the result can be recast as

$$p(t,x)=-\frac{4}{\pi}\sqrt{\frac{1-x}{1+x}}\int_{-1}^{1}\frac{v(t-\zeta-1)}{\sqrt{1-\zeta^2}}\,d\zeta+\frac{2}{\pi}\sqrt{\frac{1-x}{1+x}}\int_1^{1+t}\frac{\mathrm{d}\mu_{\mathrm{TE}}(t-\zeta+1)}{\mathrm{d}t}\frac{\mathrm{d}\zeta}{\sqrt{\zeta^2-1}}. \tag{B.14}$$

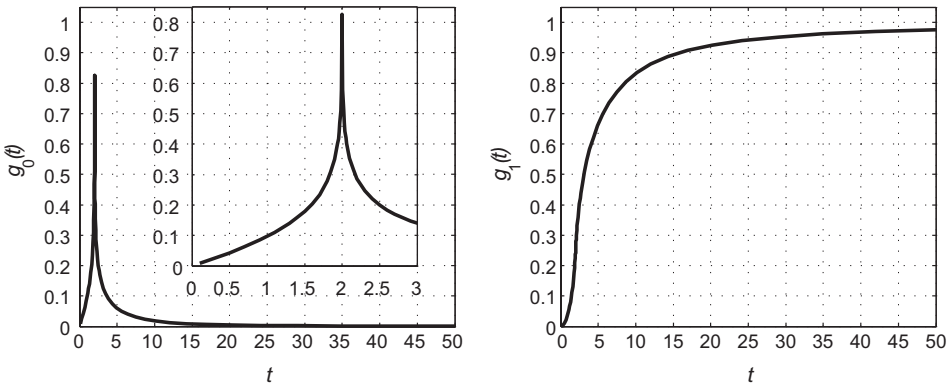

Fig. B1. Functions g_0 and g_1.

The right-most term in Eq. (B.14) can be manipulated in the same manner as the corresponding term in Eq. (28); it yields

$$p(t,x) = -4\sqrt{\frac{1-x}{1+x}}\left(\frac{1}{\pi}\int_{-1}^{1}\frac{v(t-\zeta-1)}{\sqrt{1-\zeta^2}}\mathrm{d}\zeta - \int_0^t p_0(t-\tau)v(\tau)\mathrm{d}\tau\right) \tag{B.15}$$

by (B.8). Here, $p_0(t) = L^{-1}\{\hat{p}_0; t\}$ is the inverse transform of

$$\hat{p}_0(s) = \mathrm{e}^{-s}(\mathrm{I}_0(s) - \mathrm{I}_1(s))\frac{\mathrm{K}_0(s)}{\mathrm{K}_0(s)+\mathrm{K}_1(s)}; \tag{B.16}$$

our (temporary) use of zero order response comes to facilitate subsequent derivations.

Now, using the identity

$$\mathrm{I}_0(s)\mathrm{K}_1(s) + \mathrm{I}_1(s)\mathrm{K}_0(s) = \frac{1}{s}, \tag{B.17}$$

relating the pertinent Bessel functions—see, for example, Gradshteyn and Ryzhik (1980, Art. 8.477.2)—it immediately follows that

$$\hat{p}_0(s) = \mathrm{e}^{-s}\mathrm{I}_0(s) - \frac{\mathrm{e}^{-s}}{s}\frac{1}{\mathrm{K}_0(s)+\mathrm{K}_1(s)} = \mathrm{e}^{-s}\mathrm{I}_0(s) - \hat{G}_0(s) \tag{B.18}$$

by Eq. (18). Hence,

$$p_0(t) = -G_0(t) + \frac{1}{2\pi\mathrm{i}}\int_{\gamma-\mathrm{i}\infty}^{\gamma+\mathrm{i}\infty}\mathrm{e}^{s(t-1)}\mathrm{I}_0(s)\mathrm{d}s \tag{B.19}$$

The last term here can be simplified by using integral representation of I_0,

$$\mathrm{I}_0(s) = \frac{\mathrm{e}^s}{\pi}\int_0^2\frac{\mathrm{e}^{-sx}\mathrm{d}x}{\sqrt{x(2-x)}}, \tag{B.20}$$

see, for example, Gradshteyn and Ryzhik (1980,Art. 3.364.1); upon exchanging the order of integration one should find no difficulty to obtain

$$\begin{aligned} p_0(t) &= -G_0(t) + \frac{1}{\pi}\int_0^2\frac{\mathrm{d}x}{\sqrt{x(2-x)}}\left(\frac{1}{2\pi\mathrm{i}}\int_{\gamma-\mathrm{i}\infty}^{\gamma+\mathrm{i}\infty}\mathrm{e}^{s(t-x)}\mathrm{d}s\right) \\ &= -G_0(t) + \frac{1}{\pi}\int_0^2\frac{\delta(t-x)\mathrm{d}x}{\sqrt{x(2-x)}} = -G_0(t) + \frac{1-\mathscr{H}(t-2)}{\pi\sqrt{t(2-t)}}. \end{aligned} \tag{B.21}$$

Therefore,

$$p(t) = -4\sqrt{\frac{1-x}{1+x}}\left(\int_0^t G_0(\tau)v(t-\tau)\mathrm{d}\tau + \frac{1}{\pi}\int_{-1}^{1}\frac{v(t-\zeta-1)}{\sqrt{1-\zeta^2}}\mathrm{d}\zeta - \frac{1}{\pi}\int_0^t \frac{1-\mathscr{H}(\tau-2)}{\sqrt{\tau(2-\tau)}}v(t-\tau)\mathrm{d}\tau\right). \tag{B.22}$$

But $(1-\mathscr{H}(\tau-2))v(t-\tau)=0$ for any $\tau>t$ or any $\tau>2$ by Eq. (B.2); hence the upper limit in the right-most integral can be replaced by 2; hence the last two integrals in Eq. (B.22) cancel each other. The result is

$$p(t,x) = -4\sqrt{\frac{1-x}{1+x}}\int_0^t G_0(\tau)v(t-\tau)\mathrm{d}\tau = -4\sqrt{\frac{1-x}{1+x}}\int_0^t G_n(t-\tau)\frac{\mathrm{d}^n v(\tau)}{\mathrm{d}\tau^n}\mathrm{d}\tau, \tag{B.23}$$

by analogy with Eq. (20). Consequently,

$$F(t,a) = 2\left(\int_0^t G_n(t-\tau)\frac{\mathrm{d}^n v(\tau)}{\mathrm{d}\tau^n}\mathrm{d}\tau\right)\int_a^1\sqrt{\frac{1-x}{1+x}}\mathrm{d}x = 2\left(\cos^{-1}a - \sqrt{1-a^2}\right)\int_0^t G_n(t-\tau)\frac{\mathrm{d}^n v(\tau)}{\mathrm{d}\tau^n}\mathrm{d}\tau \tag{B.24}$$

by Eqs. (39) and (A.9), whereas

$$M(t,a,h) = -\left(\int_0^t G_n(t-\tau)\frac{\mathrm{d}^n v(\tau)}{\mathrm{d}\tau^n}\mathrm{d}\tau\right)\int_a^1\sqrt{\frac{1-x}{1+x}}(x-h)\mathrm{d}x = F(t,a)\left(\frac{2h+1}{4} - \frac{(1-a)\sqrt{1-a^2}}{4\left(\cos^{-1}a - \sqrt{1-a^2}\right)}\right) \tag{B.25}$$

by Eqs. (40), (A.10) and (B.24).

Appendix C. Forces and moments

Throughout this Appendix, a and b are any real numbers in the interval (-1, 1), Qs have been defined in Eqs. (49)–(54); Λ_1 is a function that has been defined in Eq. (25); angular brackets are used to imply truncation of the negative values, i.e. $\langle x\rangle = x\mathscr{H}(x)$; and, finally, S_b^n is a function on $[-1,1]$, such that $S_b^n(x) = \langle x-b\rangle^n$. Pertinent integrals are

$$Q_{\mathrm{T}}^{(0)}\{S_b^0;a\} = \frac{2}{\pi}(b-a)\Lambda_1(a,b) - \frac{2}{\pi}\left(\sqrt{1-a^2}\cos^{-1}b - \sqrt{1-b^2}\cos^{-1}a - \cos^{-1}a\cos^{-1}b\right), \tag{C.1}$$

$$\begin{aligned} Q_{\mathrm{T}}^{(0)}\{S_b^1;a\} = &-\frac{1}{\pi}\left((b-a)^2\Lambda_1(a,b) + \sqrt{1-a^2}\sqrt{1-b^2}\right) + \frac{1}{\pi}(1-2b)\cos^{-1}a\cos^{-1}b \\ &+\frac{1}{\pi}\left((2b-a)\sqrt{1-a^2}\cos^{-1}b + (2-b)\sqrt{1-b^2}\cos^{-1}a\right), \end{aligned} \tag{C.2}$$

$$\begin{aligned} Q_{\dot{\mathrm{T}}}^{(0)}\{S_b^0;a\} = &-\frac{1}{\pi}\left((b-a)^2\Lambda_1(a,b) - \sqrt{1-a^2}\sqrt{1-b^2}\right) \\ &-\frac{1}{\pi}\left(a\sqrt{1-a^2}\cos^{-1}b + b\sqrt{1-b^2}\cos^{-1}a - \cos^{-1}a\cos^{-1}b\right), \end{aligned} \tag{C.3}$$

$$\begin{aligned} Q_{\dot{\mathrm{T}}}^{(0)}\{S_b^1;a\} = &\frac{1}{3\pi}\left((b-a)^3\Lambda_1(a,b) - (a+2b)\sqrt{1-a^2}\sqrt{1-b^2}\right) - \frac{1}{\pi}b\cos^{-1}a\cos^{-1}b \\ &+\frac{1}{3\pi}\left((1-a^2+3ab)\sqrt{1-a^2}\cos^{-1}b + (2+b^2)\sqrt{1-b^2}\cos^{-1}a\right), \end{aligned} \tag{C.4}$$

$$Q_{\widehat{T}}^{(0)}\{S_b^0;a\} = -\frac{2}{\pi}\left(\cos^{-1}b + \sqrt{1-b^2}\right)\left(\cos^{-1}a - \sqrt{1-a^2}\right), \tag{C.5}$$

$$Q_{\widehat{T}}^{(0)}\{S_b^1;a\} = \frac{1}{\pi}\left((2b-1)\cos^{-1}b - (2-b)\sqrt{1-b^2}\right)\left(\cos^{-1}a - \sqrt{1-a^2}\right), \tag{C.6}$$

$$\begin{aligned} Q_{\mathrm{T}}^{(1)}\{S_b^0;a\} = &\frac{1}{2\pi}\left((a^2-b^2)\Lambda_1(a,b) - \sqrt{1-a^2}\sqrt{1-b^2}\right) \\ &+\frac{1}{2\pi}\left((a-2)\sqrt{1-a^2}\cos^{-1}b - b\sqrt{1-b^2}\cos^{-1}a + \cos^{-1}a\cos^{-1}b\right), \end{aligned} \tag{C.7}$$

$$Q_{\Gamma}^{(1)}\{S_b^1;a\} = \frac{1}{6\pi}\Big((b+2a)(b-a)^2\Lambda_1(a,b) - (2a+b-6)\sqrt{1-a^2}\sqrt{1-b^2}\Big) + \frac{1}{6\pi}\Big(\big(2a^2-3ba+6b-2\big)\sqrt{1-a^2}\cos^{-1}b + \big(2+b^2\big)\sqrt{1-b^2}\cos^{-1}a\Big) - \frac{1}{2\pi}b\cos^{-1}a\cos^{-1}b, \tag{C.8}$$

$$Q_{\dot{\Gamma}}^{(1)}\{S_b^0;a\} = \frac{1}{6\pi}\Big((b+2a)(b-a)^2\Lambda_1(a,b) - (a-b)\sqrt{1-a^2}\sqrt{1-b^2}\Big) + \frac{1}{6\pi}\Big(\big(2a^2-2\big)\sqrt{1-a^2}\cos^{-1}b - \big(1-b^2\big)\sqrt{1-b^2}\cos^{-1}a\Big), \tag{C.9}$$

$$Q_{\dot{\Gamma}}^{(1)}\{S_b^1;a\} = -\frac{1}{24\pi}(b+3a)(b-a)^3\Lambda_1(a,b) - \frac{1}{48\pi}\big(2b^2-6a^2-5ab+12\big)\sqrt{1-a^2}\sqrt{1-b^2} + \frac{1}{48\pi}\big(16a^2b-6a^3+3a-16b\big)\sqrt{1-a^2}\cos^{-1}b + \frac{1}{48\pi}\big(2b^3-5b\big)\sqrt{1-b^2}\cos^{-1}a + \frac{1}{16\pi}\cos^{-1}a\cos^{-1}b, \tag{C.10}$$

$$Q_{\widehat{\Gamma}}^{(1)}\{S_b^0;a\} = -\frac{1}{2\pi}\Big(\cos^{-1}b + \sqrt{1-b^2}\Big)\Big(\cos^{-1}a - (2-a)\sqrt{1-a^2}\Big), \tag{C.11}$$

$$Q_{\widehat{\Gamma}}^{(1)}\{S_b^1;a\} = \frac{1}{4\pi}\Big((2b-1)\cos^{-1}b - (2-b)\sqrt{1-b^2}\Big)\Big(\cos^{-1}a - (2-a)\sqrt{1-a^2}\Big). \tag{C.12}$$

References

Ashley, H., Landahl, M., 1985. Aerodynamics of Wings and Bodies. Dover, New York, pp. 91–93, 255.

Bisplinghoff, R.L., Ashley, H., Halfman, R.L., 1996. Aeroelasticity. Dover, New York, pp. 273–281.

Bisplinghoff, R.L., Ashley, H., 1975. Principles of Aeroelasticity. Dover, New York, pp. 104–106, 114–120.

Dowell, E.H., Curtiss Jr., H.C., Scanlan, R.H., Sisto, F., 1989. A Modern Course on Aeroelasticity. Kluwer Academic Publishers, Dordrecht, pp. 212–230.

Duncan, W.J., Collar, A.R., 1932. Calculation of the resistance derivatives of the flutter theory. Advisory committee on Aeronautics, London R&M 1500.

Edwards, J.W., Ashley, H., Breakwell, J.V., 1979. Unsteady aerodynamic modeling for arbitrary motions. AIAA Journal 17, 365–374.

Edwards, J.W., 1979. Application of Laplace transform methods to airfoil motion and stability calculations. AIAA Paper, 79–0772.

Etkin, B., Reid, L.D., 1996. Dynamics of Flight. Stability and Control, New York, p. 42.

Glauert, H., 1929. The Force and Moment on an Oscillating Airfoil. Advisory committee on Aeronautics, London R&M 1242.

Gradshteyn, I.S., Ryzhik, I.M., 1980. Table of Integrals, Series, and Products. Academic Press, Orlando, pp. 311–951.

Hodgkinson, J., 1998. Aircraft Handling Qualities. AIAA Educational series, Oxford, pp. 67, 125–127.

Jones, W.P., 1941. Aerodynamic forces on an oscillating aerofoil-aileron-tab combination. Advisory committee on Aeronautics, London R&M 1948.

Jones, W.P., 1945. Aerodynamic forces on wings in non-uniform motion. Advisory committee on Aeronautics, London R&M 2117.

Jones, W.P. (Ed.), 1960. Manual on Aeroelasticity, Part 2. AGARD, Paris.

Küssner, H.G., 1936. Zusammenfassender bericht über den instationären auftreib von flügeln. Luftfahrtforschung 13 (12).

Küssner, H.G., Schwarz, L., 1941. The oscillating wing with aerodynamically balanced elevator. NACA T.M 991.

LePage, W., 1980. Complex Variables and the Laplace Transform for Engineers. Dover, New York.

Many authors, 2000, Project program: Affordable digital fly-by-wire flight control system for small commercial aircraft—second phase (ADFCS-II), EU V Framework GROWTH Project GRD1-2000-25261.

Schwarz, L., 1940. Berechnung der druckverteilung einer harmonisch sich verforme-nden tregflache in ebener stomung. Luftfahrtforschung 17 (11 & 12).

Sears, W.R., 1940. Operational methods in the theory of airfoils in non-uniform motion. Journal of the Franklin Institute 230 (1), 95–111.

Söhngen, H., 1939. Ie lösungen der integralgleihung und deren anwendung in der tragflügel-theorie. Mathematische Zeitschrift 45, 245–264.

Söhngen, H., 1940. Lift distribution corresponding to an arbitrary non-steady motion (2-dimensional). Luftfahrtforschung 17, 1446 R.T.P. Translation.

Theodorsen, T., 1935. General theory of aerodynamic instability and the mechanism of flutter. NACA Report No. 496

Theodorsen, T., Garrick, I.E., 1942. Nonstationary flow about a wing-aileron-tab combination including aerodynamic balance, NACA Report No. 736

von Karman, T., Sears, W.R., 1938. Airfoil theory in non-uniform motion. Journal of the Aeronautical Sciences 5, 379–390.

Wagner, H., 1925. Über die entstehung des dynamischen auftreiebes von tragflügeln. Zeitschrift für angewandte Mathematik und Mechanik 5 (1), 17–35.